International Journal of Applied Earth Observations and Geoinformation 112 (2022) 102833

Contents lists available at ScienceDirect

International Journal of Applied Earth Observations and Geoinformation

journal homepage: www.elsevier.com/locate/jag

Road extraction in remote sensing data: A survey

Ziyi Chen [a], Liai Deng [a], Yuhua Luo [a], Dilong Li [a,*], José Marcato Junior [b], Wesley Nunes Gonçalves [b], Abdul Awal Md Nurunnabi [c], Jonathan Li [d], Cheng Wang [e], Deren Li [f]

[a] Department of Computer Science and Technology, Fujian Key Laboratory of Big Data Intelligence and Security, Xiamen Key Laboratory of Computer Vision and Pattern Recognition, Jimei Road 668, Huaqiao University, Xiamen, Fujian 361021, China
[b] Faculty of Engineering, Architecture and Urbanism and Geography, Federal University of Mato Grosso do Sul, Campo Grande, Mato Grosso do Sul, Brazil
[c] Department of Geodesy and Geospatial Engineering, University of Luxembourg, L-1359, Luxembourg
[d] Department of Geography and Environmental Management, University of Waterloo, Waterloo, Ontario N2L 3G1, Canada
[e] School of Informatics, Xiamen University, Xiamen, FJ 361005, China
[f] State Key Laboratory of Information Engineering in Surveying, Mapping and Remote Sensing, Wuhan University, Wuhan, HB 430079, China

ARTICLE INFO

Keywords:
Road extraction
Review
2D and 3D
Remote sensing
Point clouds

ABSTRACT

Automated extraction of roads from remotely sensed data come forth various usages ranging from digital twins for smart cities, intelligent transportation, urban planning, autonomous driving, to emergency management. Many studies have focused on promoting the progress of methods for automated road extraction from aerial and satellite optical images, synthetic aperture radar (SAR) images, and LiDAR point clouds. In the past 10 years, no a more comprehensive survey on this topic could be found in literature. This paper attempts to provide a comprehensive survey on road extraction methods that use 2D earth observing images and 3D LiDAR point clouds. In this review, we first present a tree-structure that separate the literature into 2D and 3D. Then, further methodologies level classification is demonstrated both in 2D and 3D. In 2D and 3D, we introduce and analyze the literature published in the last ten years. Except for the methodologies, we also review the aspects of data commonly used. Finally, this paper explores the existing challenges and future trends.

1. Introduction

Automated road information acquisition from remotely sensed data is always an interesting research area due to its promising values in various applications, e.g., autonomous driving (Wei et al., 2020; Yang et al., 2020), road network mapping making (Senthilnath et al., 2020), road network planning (Wang et al., 2021c; Zhang et al., 2020), traffic control and management (Zhou et al., 2020), map navigation and smart city construction (Chen et al., 2021b; Tan et al., 2020), etc. Here, we considered as remote sensing data the two most popular kinds of source data, i.e., 2D earth observing images and 3D LiDAR point clouds.

Many researchers have focused their study on road extraction in remote sensing data and achieved plenty of satisfactory effects (Lian et al., 2020; Tao et al., 2019; Zhang et al., 2019c). When using Google Scholar and Web of Science as search engines, more than 450 journal papers were found out. After our review and a preliminary analysis of the titles, abstracts and methods of the found papers, about 240 study papers covering road extraction from remote sensing data since 2010 were considered in this paper. Since many research results have been presented, a comprehensive review of the published works is necessary to give a research overview, analyze the challenges, and point out the future trends.

We also search reviews about road extraction from remote sensing data, and six papers have been found since 2020. Although the six papers have focused on the road extraction review, most of them only pay attention to 2D images. 2D earth observations-based and 3D point clouds-based road information acquisition has great meanings nowadays. 2D remote sensing images are perceptual intuition in vision and lack of depth information, while in 3D point clouds data, depth information is available. Therefore, road information learning from 3D point clouds is also a popular hot research topic. However, very few reviews both cover the comprehensive works about road extraction in 2D earth observed images and 3D point clouds. Besides, a comprehensive road extraction review covering both 2D remote sensing images and 3D point clouds can give readers a better understanding of the challenges and future study trends. For the above purpose, we write this review.

The major contributions of this review paper lie on:

* Corresponding author.
E-mail address: scholar.dll@hqu.edu.cn (D. Li).

https://doi.org/10.1016/j.jag.2022.102833
Received 8 March 2022; Received in revised form 30 April 2022; Accepted 19 May 2022

- covering the road extraction reviews from a wider perspective in terms of both 2D remote sensing images and 3D point clouds;
- providing a comprehensive review of the 2D and 3D remote sensing datasets commonly used for research about road information acquisition;
- presenting a detail analysis of challenges and future trends of road extraction from remote sensing data.

The rest of this paper is organized as follows. Section 2 gives a short overview of this review. In section 3, the detail review papers are illustrated from three aspects: road extraction from 2D, 3D and 3D&2D. We also give a brief introduction about commonly used and publicly available 2D and 3D data sets for road extraction in Section 4. Section 5 reviews the performances of methods among data sets in Section 4. The observed trends and opportunities are analyzed in Section 6. Finally, we come to a conclusion in Section 7.

2. Short overview

Fig. 1 presents the tree structure of research fields in road extraction from both 2D earth observed images and 3D point clouds. This review first separates the road extraction from 2D earth observed images and 3D point clouds, respectively. Further, the road extraction from 2D earth observed images is classified into three image types: SAR images based, optical images based, and fusion of SAR and optical images based. Besides, the road targets in 2D earth observed images are further classified into road areas and road lines (including centerlines and boundary lines). The road extraction from 3D point clouds in this review includes three types of methods: MLS-based, ALS-based, and TLS-based. In all three types, most methods fall in the category of road geometric shape-based and data characteristics-based.

To investigate the paper publication trend of research about road information acquisition from 2D earth observed images and 3D point clouds, we also figure out the publication numbers of each year in the last ten years. Figs. 2 and 3 show the number of papers on road extraction in the last ten years for 2D and 3D data, respectively. From those two figures, we can see that the research about road information acquisition from remote sensing data is becoming hotter. The reason may be the rapid development of urbanization, resulting to paying attention to the city road network planning, proper traffic management, emergency rescue, etc. We also analyze the word cloud of paper titles reviewed by this paper, as shown in Fig. 4. From Fig. 4, we see that some words appear with high frequency, such as “high-resolution”, “neural network”, “VHR”, “Deep Learning”, etc. These high-frequency words show the research hot points in the current road extraction from remotely sensed data, helping the researchers to better position and focus on the current suitable research areas.

3. Method

3.1. Road extraction by 2D remotely sensed data

Road extraction from 2D remotely sensed data usually use two kinds of image sources: (1) optical ones, and (2) SAR images. They possess rather different characteristics. To make the outline of our review clearer for readers, we separated the road extraction by 2D remotely sensed data into two parts, namely optical remote sensing image-based and SAR image-based.

3.1.1. Road extraction from optical remote sensing images

Using optical earth observed images, three road elements are the major extraction targets, namely road areas, road centerlines, and road boundaries. Further, in the extraction methodologies for all three road elements, three kinds of methods can be observed, (i) morphological feature-based, (ii) handcrafted feature-based, and (iii) automatic feature extraction-based, i.e. deep learning-based. Thus, we will introduce the related work about road extraction from 2D remotely sensed data according to the extraction elements. Then, in the introduction to each road extraction element, we will illustrate the related works according to the three methodological classifications. It should be noted that we only introduce the most related works published in the last ten years.

(1) Road Area Extraction.

We first present a chronological overview of the most relevant methods, shown in Fig. 5. Then, we review approximately according to Fig. 5.

Road area extraction methods extract road pixels from the whole image and classify the pixels as “roads” or “non-roads” (Bastani et al., 2018; Chen et al., 2020). Usually, road areas are covered by other

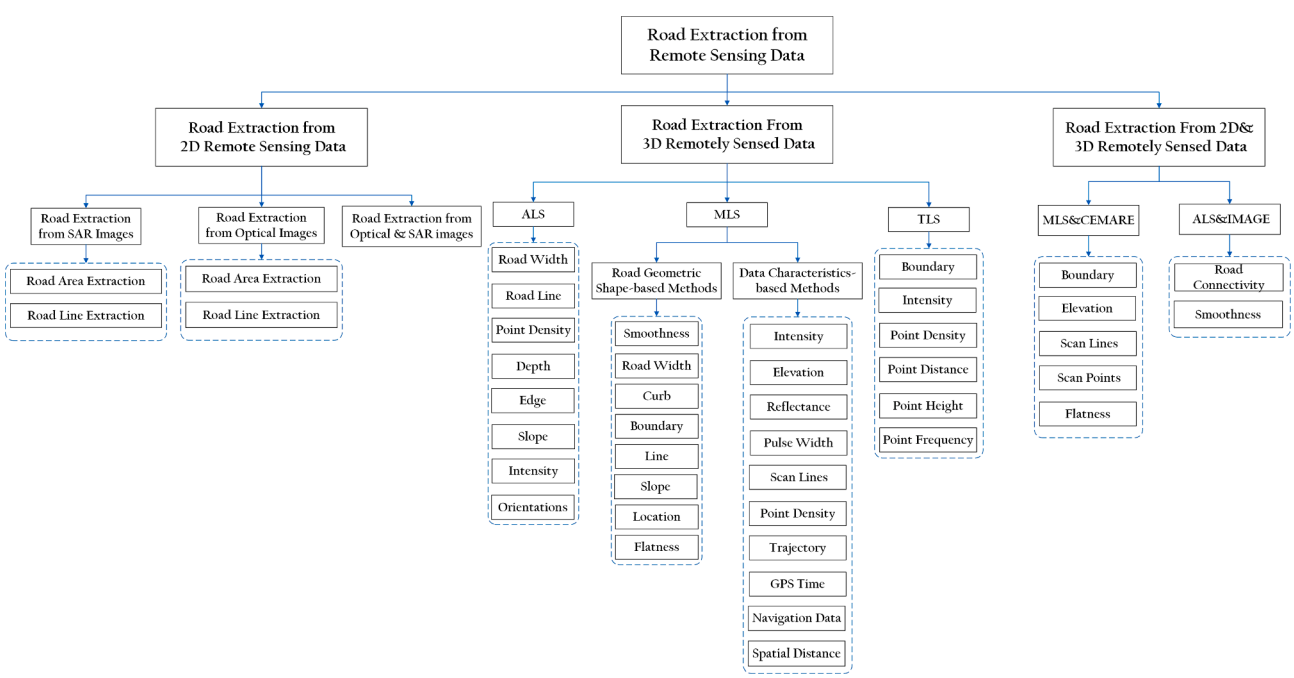

Fig. 1. Tree structure of the study areas in road extraction from 2D and 3D remote sensing data.

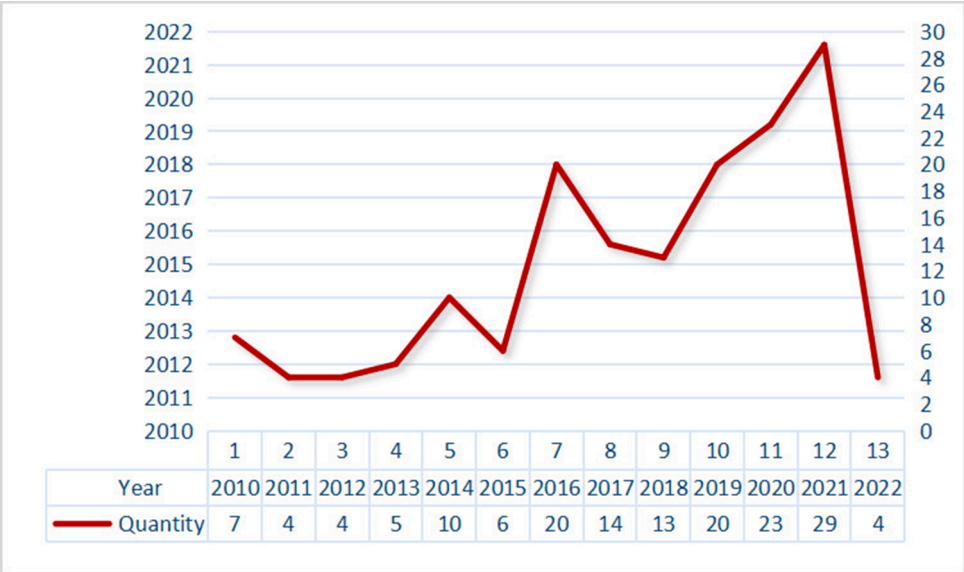

Fig. 2. Publication paper numbers in the last ten years about road information learning from 2D earth observed images. Line diagram reveals increasing number of publications of road extraction (from 2D data) for almost every year in past 10 years.

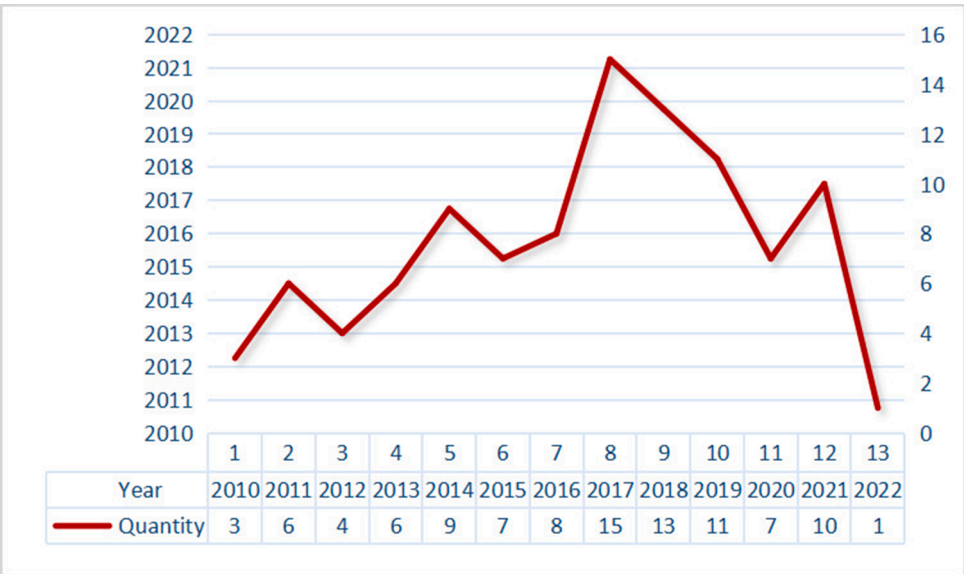

Fig. 3. Number of publications in past 10 years about road extraction from 3D point clouds.

ground object shelters, e.g. cars, trucks, buses, motorcycles, etc. Among our review, those road ground shelters are treated as road areas in the labels. Although road area object shelters may make the road areas complex, they also can provide important context information, benefiting for the road area recognition under complex situations.

Since road areas usually present related constant shape and appearance features, morphological features have wide usages (Alshehhi and Marpu, 2017). Common morphological features include features of shapes, widths, etc. To obtain the morphological features, the operations of binarization, expansion, erosion, opening and closing are usually applied.

When using morphological features, a preferred shape-biases may be introduced. To solve this issue, Valero et al. (2010) proposed an advanced directional morphological operators, which introduced the Path Openings and Path Closings. Chaudhuri et al. (2012) proposed customized operators to exploit the road directional and morphological attributes. A low- and high-level processing was proposed for road extraction in (Bae et al., 2015), which used widths, contrast properties, orientations, lengths, and a graph cut-based classifier. A geometric active deformable model based on width and color was proposed in (Leninisha and Vani, 2015). Unlike normal morphological filters directly computed on pixels, the morphological path filters are applied to regions in (Courtrai and Lefèvre, 2016). Grinias et al. (2016) proposed an unsupervised method using shape features that were combined with the Markov random field model and the Random Forest method to cluster road likelihoods. Zang et al. (2017) proposed a specially designed pixel value-based enhancement approach.

Morphological feature-based methods can effectively obtain the road shape features, however, these methods usually suffer from a lack of robustness to occlusions, light and contrast variations. The handcrafted features are texture features that satisfy special constraints. The handcrafted features usually rely on manually designed operators. After features are extracted, classifiers are followed for final classifications. The classical classifiers include decision tree, support vector machine

Fig. 4. Word cloud of paper titles reviewed by this paper.

(SVM), Hough Forest, Tensor Voting, etc. Handcrafted features have achieved much success in this survey section (Krylov and Nelson, 2014; Poullis and You, 2010; Wegner et al., 2015).

A ridge- or ribbon-like linear feature highlights the potential road areas in a remote sensing image. Shao et al. (2011) extracted ridge- or ribbon-like linear features, then classified a pixel as road or not, based on its grey value and the position relationships with linear features. Movaghati et al. (2010) treated the road network extraction as a tracking task using handcrafted features. Das et al. (2011) proposed a multistage framework, which used four Probabilities SVM combined with Dominant Singular Measure to detect potential roads. Different from pixel-based processing, Wegner et al. (2013) extracted road areas based on superpixels. The color and texture features combined with a 17-dimensional Gaussian filter band were used for feature representation of each superpixel. Different feature extraction methods were combined for a more robust feature representation of road in (Poullis, 2014). The tensor coding and Gabor Jets were used to extract various types of features, including surfaces, curves, and joints. The object-based strategy with five steps was proposed in (Miao et al., 2015). In (Hormese and Saravanan, 2016), the road extraction framework included image smoothing, feature extraction, continuity judgment, and vector representation of roads. Li et al. (2016b) proposed a method based on a Binary Partition Tree, combining two geometric features, two orientation histogram-based structural features, and morphological profiles using a series of path openings. Maboudi et al. (2016) used a context-aware feature integration strategy to extract road features and tensor voting to classify the pixels into the road and not road areas. The contextual feature integration strategy extracted structure features, spectral features, and textual features. Sghaier and Lepage (2016) proposed a framework through texture analysis and Beamlet Transform. The direction information was embedded into ant colony optimization in (Yin et al., 2016). Two kinds of features were extracted, namely FNEA (fractal net evolution approach) for geometric feature extraction and EDISON for edge feature extraction. Zhang et al. (2016) proposed a framework by combining morphological operations, manual edge feature extraction, geometric feature extraction, and tensor voting. Bakhtiari et al. proposed a method based on edge attributes and SVM in (Bakhtiari et al., 2017). To improve performance and reduce the false alarms of road extraction from images under disaster situations, a method based on the Lowe's scale-invariant features (SIFT) and spectral angle algorithm were proposed in (Coulibaly et al., 2017). The sparse representation was used in (Lv et al., 2017), which joint multiple sparse features, including sparse representation features, color features, local entropy features, and HSC features. Histogram of oriented gradient (HOG) feature was combined with SVM for road extraction from remote sensing images in (Zhang et al., 2017). Zhou et al. used the stroke width transformation (SWT) feature in (Zhou et al., 2017). After the extraction of SWT features, they were used in a clustering algorithm and connected component analysis. Ziems et al. used multiple road extraction models for road extraction in (Ziems et al., 2017). The input images were separated into individual channels and gray value channel, based on which multiple road extraction modules were computed. The multiple modules included line detection, color classification, low vegetation detection, adjacency analysis, edge detection and building detection. Alshehhi et al. proposed a hierarchical graph-based approach in (Alshehhi and Marpu, 2017). The Gabor and morphological filters were combined for feature extraction. A two-stage approach was proposed to increase the ability to find weak road edges and avoid noise in (Chen et al., 2018b). Maboudi

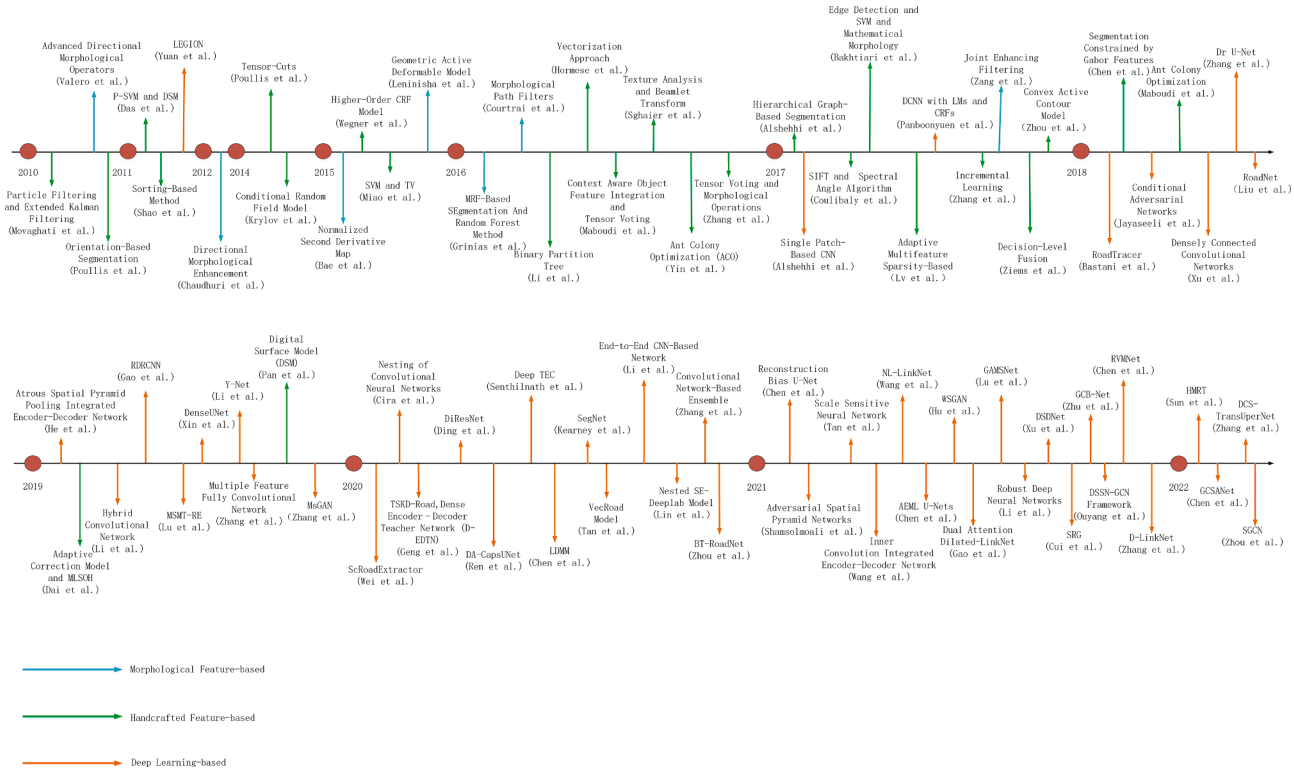

Fig. 5. Chronological overview of our reviewed papers about road area extraction from optical remote sensing images.

et al. proposed a road extraction method that incorporates spatial, spectral and textural object features, feeding to the fuzzy logic system for handling the uncertainties (Maboudi et al., 2018). To enhance the feature representation, a multi-scale line segmentation orientation histogram (MLSOH) feature, sector feature and multiple angle Beamlet feature were used for feature representation in (Dai et al., 2019). The entropy and spectral features and information from the digital surface model (DSM) were combined as feature representation in (Pan et al., 2019).

Handcrafted feature-based methods can usually perform more robustly than methods based on morphological features. However, handcrafted feature-based methods still suffer from the challenges of occlusions, weak extendibility for the different data sources, and the difficulty in best parameter selections. Recently, many computer vision-related jobs has achieved great breakthroughs with the development of deep learning, which has also obtained much success in the survey topic of this review (Kestur et al., 2018; Zhang et al., 2018c).

The earliest neural network-based road extraction method in the last ten years in our review is the work proposed by Yuan et al. (2011), which designed a network named LEGION to stimulate local and suppress global. The deep learning-based methods have gap years between 2011 and 2017, during which few deep learning-based road extraction work was presented. Then, they have had an outbreak period since 2017.

Most of the deep learning-based methods can be separated into convolutional neural network (CNN) based (Chen et al., 2020; Liu et al., 2018), fully convolutional neural network (FCN) (Wang et al., 2018; Zhang et al., 2019c), U-Net based (Ren et al., 2020; Wang et al., 2021c) and generative adversarial network (GAN) based (Shamsolmoali et al., 2021;Zhang et al., 2019b).

For CNN-based methods, commonly, the pixel-by-pixel processing strategy is used. The segmentation results usually present high accuracy, while the processing speed of CNN methods is usually slower compared to FCN and U-Net based methods. Alshehhi et al. (2017) proposed a CNN based model to simultaneously extract road areas and building footprints. In (Alshehhi et al., 2017), low-level features of roads and buildings were combined with CNN features to further improve the performance. Bastani et al. (2018) proposed a RoadTracer which contains two CNN models: one was utilized to detect which pixel belonged to a road, and another was used to make the decision on the construction of the road network map. A multi-task CNN called RoadNet was proposed in (Liu et al., 2018), which learns to simultaneously output road surfaces, centerlines and edges. Chen et al. combined unsupervised model named LDMM and CNN models in (Chen et al., 2020). Cira et al. classified secondary roads in (Cira et al., 2020), which integrates three CNN architectures (VGG, ResNet and Inception-ResNet). Gui et al. used CNN as feature extractor first, then a superpixel based graph CNN was applied for road extraction (Cui et al., 2021). Sun et al used multi-resolution transformer CNN to enlarge the reception field of the network, showing good results in the experiments (Sun et al., 2022). To learn about the multi-scale and global context information, Chen et al embedded a global context attention module into DenseNet-121 for road classification in (Chen et al., 2022).

FCN-based road extraction models use convolution layers instead of the final fully connected layers in the CNN models. Besides, FCN models usually use addition operation for feature fusion among different layers. To ensure the integrity and continuity of the extracted roads, Zhang et al. (2019c) proposed a FCN model which can extract multiple spectral and terrain features. To solve the imbalance problem of road and background areas, Zhang et al. (2020) proposed a FCN model that weights the loss function to give more importance to the road areas, which is the minority class. To reduce the cost of data labeling work, Pan et al. (2021) trained a FCN model utilizing OpenStreetMap. To both extract road pixels and connect the road breakages, Chen et al. proposed a network named RVMNet to capture the vectorization mapping in (Chen et al., 2021a). Xu et al. designed an Encoding-Decoding like FCN architecture for mountainous areas in (Xu et al., 2021).

Unlike FCN that uses addition operation for feature fusion among layers, U-Net (particular type of FCN) models usually use concatenation operation for feature fusion. U-Net usually contains two parts: encoding

and decoding, organized as a "U" shape. To use the great feature extraction power of a densely connected convolutional network (DenseNet), the DenseNet was embedded into a U-Net architecture for road extraction in (Xu et al., 2018). To alleviate the training loss degradation problem and enhance the context information learning ability, Gao et al. (2019) proposed a refined deep residual CNN model. Lu et al. (2019) treated road area extraction and road center line extraction as a multi-task problem, and designed a U-Net embedding multi-scale information. Ding and Bruzzone (2020) designed a DiResNet which the model embedded context-aware, direction-aware, and structure-aware modules into the U-Net architecture. The direction-aware strategy can help the model learn better linear road features. Ren et al. (2020) designed a DA-CapsUNet to learn the relationships among object parts. To learn the structure and junction information, Tan et al. (2020) proposed a Vec-Road model. Wei et al. designed a ScRoadExtractor model in (Wei and Ji, 2020), which used an algorithm to propagate labels from the road center scribble to nearby unlabeled pixels to reduce the labeling effort. To increase the learning ability about boundary and topological structure, Zhou et al. designed a BT-RoadNet in (Zhou et al., 2020), which is composed of two U-Net-like networks. Li et al. designed a model which used a direction-aware attention block to obtain the road topology information in (Li et al., 2020). Kearney et al. used a SegNet architecture to extract rural road network in (Kearney et al., 2020). Wang et al. (2021b) designed a U-Net that can propagate information slice-by-slice within feature maps, increasing the learning ability about topology and linear information. Wang et al. proposed a NL-LinkNet to understand the relationships between features in global in (Wang et al., 2021c). To match the encoding and decoding challenge, a reconstruction-bias idea was proposed in (Chen et al., 2021b). To release the labeling work, Zhang et al. used GPS trajectories of floating cars to label road areas, generating training data to train a D-LinkNet for urban road extraction in (Zhang et al., 2021). Li et al. (2021d) used crowd sourced data to train U-Net like models to release the hard labelling burden. To effectively use the power of different convolutional layers, Tan et al. (2021) proposed a scale-sensitive U-Net. Lu et al. (2021a) designed a GAMS-Net that contains multi-scale residual learning to capture global information. Ouyang and Li proposed a graph CNN in (Ouyang and Li, 2021), which combined the deep semantic segmentation network and graph CNN. Zhang et al. designed a U-Net like network which used a dual resolution transformer module and a feature fusion part to obtain the global context information (Zhang et al., 2022).

To fuse the advantages of models with different architectures, Li et al. (2019b) designed a hybrid network containing FCN, U-Net and VGG. Li et al. (2019a) proposed a Y-Net which combined a U-Net and a FCN. Except for the use of manual labels for training, Sun et al. (2019b) proposed a method which used crowd sourced GPS data as road area label. To reinforce the ability of dealing with occlusions by trees, shadows, etc., Zhou et al. proposed an Encoder-Decoder framework which capture features through a depth-wise graph CNN (Zhou et al., 2022). They tested on the Massachusetts Road data set and their own mountain road data set obtained by ZY-3 satellite, showing good results.

Generative Adversarial Network (GAN) contains two parts: one for generating fake samples while the other for classifying the samples as fake or true. Zhang et al. (2019b) raised a GAN-based network, which can identify challenging road areas caused by occlusions and shadows. Shamsolmoali et al. (2021) designed a GAN model that contains a feature pyramid network (FPN) module. Jayaseeli et al. (2018) incorporated the U-Net and GAN. A similar idea was used in (Senthilnath et al., 2020), which combined FCN and GAN. In (Senthilnath et al., 2020), they used a FCN, a pix2pix, and a CycleGAN to conduct the extraction, respectively. Then, the extracted results were merged through a voting classifier. Hu et al. proposed a weakly supervised process GAN (WSGAN) to extract road network in (Hu et al., 2021).

(2) Road Centerline Extraction.

Fig. 6 shows the chronological overview of the most relevant methods of road centerline extraction with optical remote sensing images. We will introduce the review works mainly according to this chronological overview.

Road centerline extraction usually uses thinning algorithms to obtain the final centerlines after potential road areas extraction. The road centerline extraction methods also can be separated into traditional machine learning-based methods and deep learning-based methods.

3.2. Traditional Machine learning based methods

Miao et al. (2014b) proposed a geodesic method, which generated probability map through propagation from a seed point. After extracting potential road areas, the road centerlines was extracted by KDE and Mean Shift. Miao et al. (2014a) used tensor voting under a classified image to obtain centerlines. In Miao's another work (Miao et al., 2013), shape, Laplace, and spectral features were used as inputs of an adaptive regression function. Shi et al. (2014a) raised an integrated method, in which the general adaptive neighborhood approach was introduced first. Then, the local Geary's C and shape features were used for improving the road segmentation results. Finally, the centerlines were extracted through a local linear kernel based regression. The local Geary's C was also used in (Shi et al., 2014b), which using spectral-spatial classification first. Then, performance was further improved by using shape features.

To reduce the impact of limited labeled samples, Cheng et al. (2016a) proposed a semi-supervised method, which exploits the intrinsic structures between the labeled and unlabeled samples. Cheng et al. (2016b) extract multi-scale representations first, then they were as the input of graph cuts. Liu et al. proposed an approach in (Liu et al., 2016) containing three steps. First, they used shear transform with directional segmentation to obtain the initial road areas. Then, the Mahalanobis

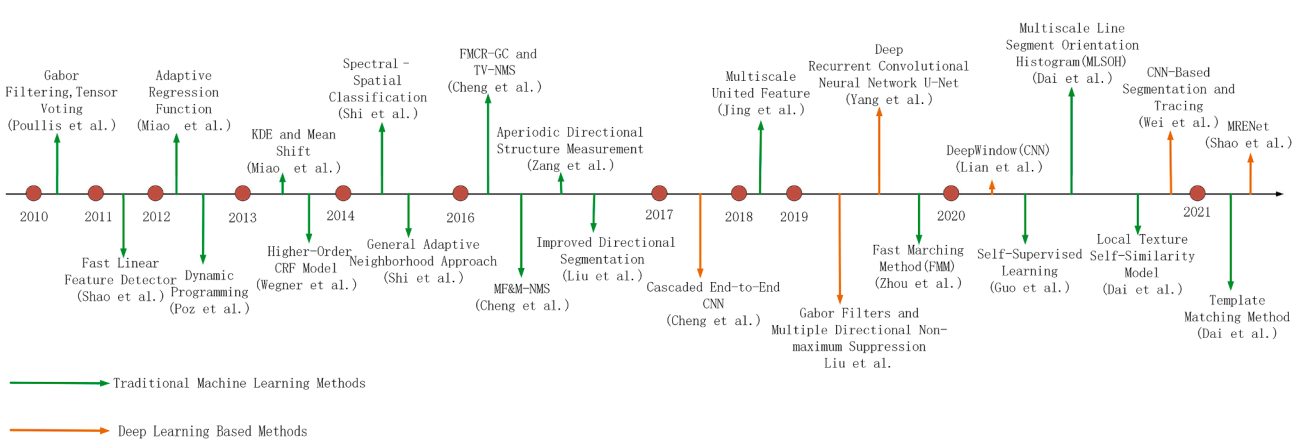

Fig. 6. Chronological overview of our reviewed papers about road centerline extraction from optical remote sensing images.

distance, thresholding, shape feature filtering, and hole filling were applied. Finally, an automatic sub-voxel skeletonization method was proposed. Zang et al. (2016) proposed an aperiodic directional structure measurement, through which a mask can construct to denote potential road areas. Jing et al. (2018) designed an approach applied under island situation using joined features in a multi-scale perspective. In their method, the joined features contain the spectral, geometric and texture information. Zhou et al. (2019) proposed a fast marching method (FMM), which obtains the distance fields first. After that, a branching-tracking technique and a tensor field were. Dai et al. (2020b) used OpenStreeMap (OSM) data to create road-poistive samples, with which to learn the attributes of roads' orientation, texture feature statistics and homogeneity. Guo and Wang (2020) designed a self-supervised learning strategy, which combined spectral and shape features as inputs to a one-class classifier and a random forest classifier to obtain posterior probabilities. After that, the tensor voting was used. Dai et al. (2021) proposed a template matching method, in which the straight lines and the geometric characteristics of narrow and long roads are used as features for road center point recognition.

3.3. Deep learning based methods

Cheng et al. (2017) designed a cascade CNN model that can simultaneously extract the road areas and road centerlines. In their model, two networks with a cascaded relationship were used to extract road areas and road centerlines, respectively. Liu et al. (2019) designed a processing flow which used a CNN model to extract the initial road areas, edge-preserving filters to improve the road area extraction, Gabor filters with multi-scale and multiple non-maximum suppression to acquire centerlines. Yang et al. (2019b) proposed a one-stage method based on the recurrent CNN with a U-Net architecture. Through the recurrent CNN module, the network increases the ability of getting rich spatial context information. Wei et al. (2020) proposed a FCN model, which used a tracing strategy starting from multiple seed points to obtain the topology of the road network. Lian and Huang (2020) proposed a DeepWindow model for road centerline extraction from the remote sensing images. The DeepWindow method also used a tracing strategy based on CNN without prior road segmentation. Shao et al. (2021) designed an MRENet with multi-task strategy which simultaneously forecast the surfaces and centerlines.

Except the road areas and centerlines, several road extraction methods from remote sensing images only detect the road boundaries. Li et al. (2010) generate road boundaries using a ridgelet transform. Recently, Liang et al. designed a model with the recurrent FCN in (Liang et al., 2019) to extract road boundaries, which combined LiDAR data and camera images as an input data source.

3.3.1. Road extraction from SAR images

Fig. 7 shows the chronological overview of the most relevant methods of road extraction from SAR images. We will survey works about road extraction from SAR images mainly according to the chronological outline.

Under this review, we separated the road extraction from SAR images into 3 groups: road area extraction based on traditional methods (Lu et al., 2014;Perciano et al., 2016;Xiao and Tong, 2019), road area extraction based on deep learning (Khesali et al., 2016) and road centerline extraction (Cheng et al., 2011;Cheng and Gao, 2016).

(1) Road area extraction

The road area extractions from SAR images based on traditional methods often use morphological features or handcrafted features to extract road features, which are combined with the classifiers to obtain the final road areas. Deng et al. (2010) raised a GVF snake model in early 2010. To obtain multi-scale information, He et al. (2012) proposed a multi-scale geometric analysis approach about detector responses. The snake model and Particle filtering were used to extract road from SAR images in (Liu et al., 2013). The multi-scale linear features were also used in (He et al., 2014) for extracting roads from SAR images. In their work, quadratic kernel for non-linear candidates was utilized to select the segmentation directions. Superpixel segmentation was used as basic extraction elements in (Koch et al., 2015), whose feature extraction was conducted based on superpixels. Mu et al. proposed a method using Zernike moments in (Mu et al., 2016). In their work, the potential areas of the road were extracted through morphological operations and Otsu thresholding. Finally, Zernike moments were used for road area classification within the previous potential areas. Jiang et al. (2017) proposed a robust framework from InSAR images. In their framework, a multi-temporal covariance matrix was proposed to estimate potential road areas, which used intensity and coherence as observations. Xu et al. (2017a) proposed a framework that main idea was using a Bayesian strategy. To effectively detect the line characteristics, a multi-scale approach was proposed. Zeng et al. (2019) proposed an algorithm that contains two steps. In the first step, a linear detector was used, in which a false edge removal algorithm was embedded using directional information. Finally, the road areas were extracted through region growing.

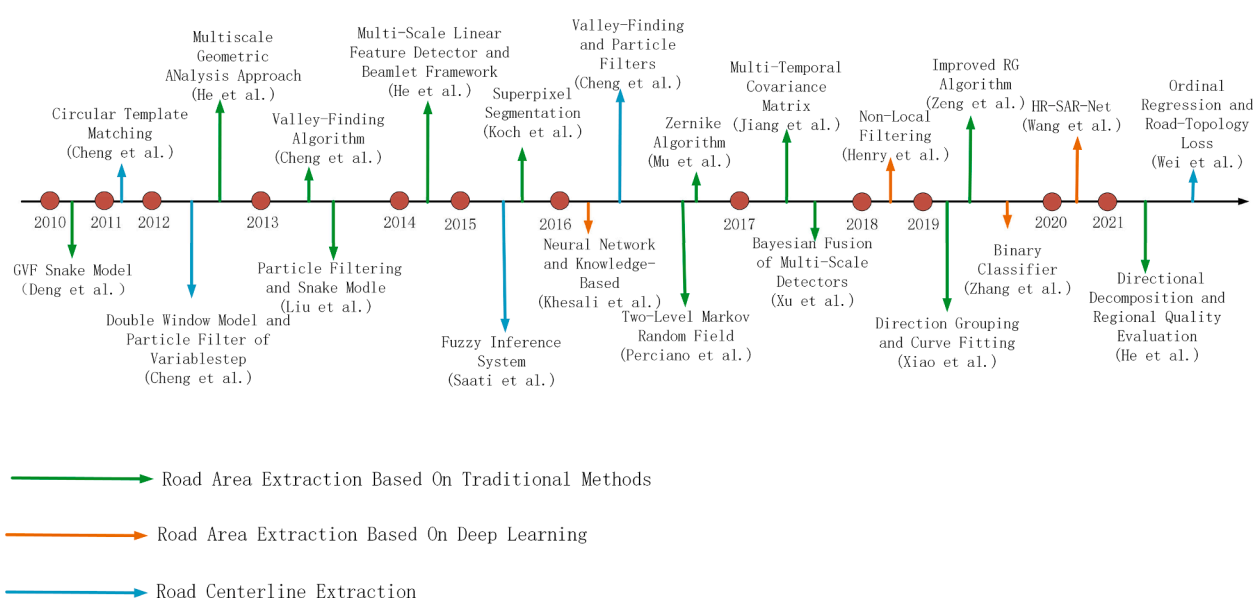

Fig. 7. Chronological overview of our reviewed papers about road extraction from SAR images.

An effective road extraction framework was proposed in (Xiao et al., 2019), which used the Uuda operation to augment the road area features and a SVM classifier to generate a non-road area mask. The potential road area segmentation, the preliminary generation and the refinement were contained in the framework of road extraction from SAR images in (He et al., 2021). In the potential road area segmentation part, the direction information with multi-scales was combined with intensity information for threshold-based road segmentation. In the second part, the multi-scale curve fitting strategy was used to generate the road network.

For road area extraction from SAR images based on deep learning, the road area representations were learned automatically through deep neural networks. Henry et al. (2018) designed a FCN based model, which also used non-local filtering for preprocessing and fully connected CRFs for post processing. Similarly, FCN was used in (Zhang et al., 2019a), which combines a binary classifier for improving the final road extraction performance. Wang et al. (2020) proposed a DNN based model through pixel-wise classification. Benefiting from the small scales of parameters, the model obtained a satisfactory processing efficiency.

(2) Road centerline extraction

Centerline extraction from SAR images also attracts the attention of many researchers. Cheng et al. (2011) proposed a semi-automatic approach with circular template matching. Cheng et al. (2012) raised an approach that using iteratively detection and tracing strategy. In (Saati et al., 2015), different radiance information was used as the features for potential road area extraction through fuzzy inference. After that, the morphology skeletonization was applied to generate seed points which formed the final road centerlines after connection. In (Cheng and Gao, 2016), road junctions were extracted using a valley-finding algorithm. Then, the centerlines were generated by particle filters with multiple seed points. Deep learning was also used in (Wei et al., 2021) for road centerline extraction from SAR images. They designed a network with a multi-task learning strategy, simultaneously extracting the road areas and centerlines.

Except for the road extraction only relying on SAR images, there are also several researches focusing on the fusion of optical and SAR images for road extraction. Poulain et al. (2010) proposed a road database updating approach through fusion the road extraction results based on optical and SAR images. In (He et al., 2013), the roads were extracted by fusing the structure information obtained in SAR images and the stereoscopic information obtained in optical images. Finally, a multi-scale geometric analysis was applied for road network grouping. Lin et al. used United U-Net (UUNet) to fuse Sentinel-1 and Sentinel-2 images to extract roads in (Lin et al., 2021). In their experiments, the UUNet obtained better results than CNN models trained with optical or SAR data alone.

3.4. Road extraction by 3D remotely sensed data

The 3D point clouds are the main 3D data source for road extraction. According to the difference of platform, 3D point clouds can be collected by mobile laser scanning (MLS), airborne laser scanning (ALS), and terrestrial laser scanning (TLS). The extraction approaches on 3D point clouds acquired from different platforms are considerably different. We further divide the approaches into three branches: road extraction by MLS, ALS, and TLS.

3.4.1. Road extraction by MLS

Fig. 8 shows the chronological overview of the most relevant methods of road extraction from MLS data. We will introduce the review work about road extraction from MLS data mainly according to the chronological outline.

Mobile LiDAR technology is currently the focus in remote sensing and laser scanning. Mobile LiDAR enables a rapid collection of enormous volumes of highly dense and accurate geo-referenced 3D point clouds along roads. Naturally, MLS technology has gained popularity in road recognition. From the aspect of the main features used for road

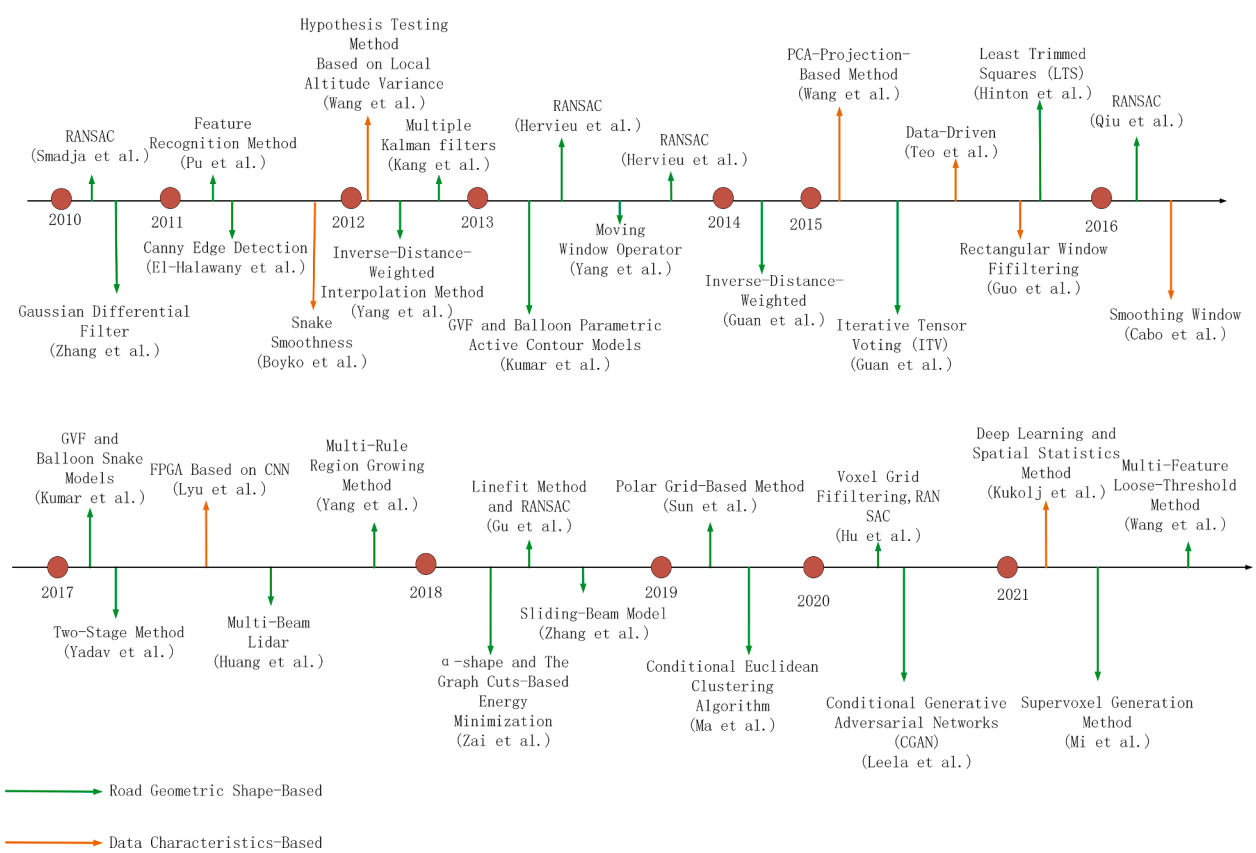

Fig. 8. Chronological overview of our reviewed papers about road extraction from MLS data.

extraction, we categorize the related approaches into two groups, (1) road geometric shape, and (2) data characteristics.

(1) Road geometric shape-based extraction.

One of the most common characteristics of road geometric shape is flatness. After ground points filtering, many methods directly extract the planar road surfaces from point clouds. Yang et al. (2017a) proposed a road facilities recognition method by combining multiple aggregation levels of features and contextual features. They first segmented the ground points, and further segmented them into several planes using RANSAC algorithm. Then, the road surface points were then recognized by two rules, which were drawn up by the trajectory data and normal vectors of road surface segments. To adapt to the complex road environment, such as rural roadways, which lack raised curbs and hard to identify the road boundary, Yadav et al. (2017) and Yadav and Singh (2017) proposed the more generalized road surface extraction methods. They first extracted the planar ground surfaces, and further extracted the road surface points by properties like topology, smoothness, point density and intensity. Zhang et al. (2018a) proposed a plane-based filtering method to recognize the road surface area. The filter constitutes a linear equation plane, and the parameters of the plane are estimated by the random sample-consensus method. Hu et al. (2020) extracted the road surface plane by using the RANSAC algorithm from ground points firstly. Then, according to the difference of density of road point set, they set the point density threshold to further extract road surface points. Pu et al. (2011) presented a framework for road inventory structure recognition. Firstly, the whole scenes of the roadside were classified into three categories with an initial rough classification. Then, a collection of geometric characteristics was used to further segment the rough classified point clouds into detailed classes, including road. Smadja et al. (2010) proposed a two-step road extraction method. The road side points were roughly estimated by using the RANSAC algorithm in the first place, then the road boundary and center points were extracted based on the road width and curvature.

Except for the flatness, smoothness or roughness are also the inherent attributes of roads that have the potential of using as features to extract road surface. Zhang (2010) used a Gaussian differential filter to select the candidate road regions, and evaluated the smoothness by the variance of the ground elevation. Then, a fixed threshold was used to detect the exacted road surface points.

Road boundary indicates the region of the road directly. Thus, by the extraction or detection of road boundary points, the precise road area could be extracted. Yang et al. (2012) proposed a street-scene objects extraction method. They generated the geo-referenced feature images from mobile LiDAR data and extracted boundaries of street-scene objects based on these images. Then, the corresponding 3D boundary points were extracted by the 2D extracted boundaries. Kumar et al. (2013) generated the 2D raster surfaces, and extracted the road boundaries by the snake model. Qiu et al. (2016) extracted a rough plane by using the RANSAC algorithm, and further extracted and refined the road edge points based on road width and continuity. Kumar et al. (2017) combined the gradient vector flow (GVF) and balloon parametric active contour or snake models to extract road edges. Zai et al. (2018) generated supervoxels by selecting smooth points as seeds and assigning points into facets centered on these seeds using several attributes, and further extracted the road boundaries using the α-shape algorithm and the graph cuts-based energy minimization algorithm. Gu et al. (2018a) preprocessed point clouds by multi-frames Iterative Closest Point (ICP) registration and VoxelGrid down-sampling, and extracted the road surface points by Linefit method and RANSAC algorithm. Sun et al. (2019a) presented a polar grid-based method to separate the ground points and non-ground points, and detected the road boundaries by the trajectory data and feature filters. Leela and Panda (2020) presented road boundary detection method by transforming the point clouds into 2D images and using conditional generative adversarial networks (CGAN). Similar to (Zai et al., 2018), Mi et al. (2021) generated supervoxels, and extracted road boundaries by clustering, fitting, tracking, and completion operation. Wang et al. (2021a) proposed a speed and accuracy tradeoff road boundary detection method. The method consists of three main stages, feature points extraction (by a multi-feature based method), feature points classification (by a road-segmentation-line-based method), and filtering out false points and extracting boundary points (by an iterative Gaussian Process Regression).

For urban roads, curbs are usually regarded as the boundary of roads. Therefore, the roads could be represented by curbs in the urban environment, and there are many studies focusing on this field, which could be classified as "curb-based road extraction methods". El-Halawany et al. (2011) segmented the ground and non-ground points by calculating eigenvalues and surface normal and detected the curb from the street floor and sidewalks using 3D and 2D techniques. Kang et al. (2012) proposed a decision-making method for road boundary detection by using multiple Kalman filters. Yang et al. (2013) partitioned the point clouds by using the GPS time and found the candidate road area by a moving window operator. Then, the curbs were detected by three rules, elevation jump, point density, and slope change. Hervieu and Soheilian proposed two roadside detection approaches by using the angle deviation to ground normal in (Hervieu and Soheilian, 2013b;Hervieu and Soheilian, 2013a). Hinton et al. (2015) introduced the least trimmed squares (LTS) instead of temporal filters and spline fitting to deal with occluding scenes, which achieved robust road curb detection results in different traffic situations. Guan et al., (2014) and Guan et al. (2015) separated the point clouds into a set of blocks by trajectory data, and extracted the road curb points by generating the pseudo scan line from each block profile. Based on (Guan et al., 2014; Guan et al., 2015), Ma et al. (2019) revised the fixed size of data blocks into the dynamically determined to achieve better extraction results. RodrguezCuenca (2015) used the point clouds and trajectory data as the input and detected the curb by the rasterization and segmentation processing. Yang et al. (2017b) proposed a road information extraction method by a 3D local feature descriptor, called the binary kernel descriptor (BKD). Huang et al. (2017) segmented the ground points, and detected the road curb by applying the global road trend and extraction-update mechanism. Xu et al. (2017b) extracted the candidate points of curbs based on the energy function, and refined the candidate points by using the least cost path model. Rato and Santos (2021) adopted the similar method as Xu et al. (2017b) used, but achieved the better performance and processing speed by using a 4-layer LiDAR to increase the ground point density. Jung et al. (2020) extracted the curb candidates based on PCA and DBSCAN, and selected the optimal candidate using an optimization framework. Huang et al. (2021) classified the road points and curb points based on the segment point density. Kukolj et al. (2021) combined deep learning and spatial statistics method to detect road edges, which recognized the point cloud segments by the pre-trained RandLA-Net and generated the edge segments by voxelization and spatial statistical analysis. Zhao et al. (2021) combined both spatial information and geometric information for complex scenes' curb extraction.

(2) Data characteristics-based extraction.

Elevation data has been widely used for ground and non-ground points separation. For road extraction, elevation and the differential of elevation are the crucial features. Guo et al. (2015) proposed a road surface reconstruction method. They extracted the road surface by using two filtering procedures, and the filters were created by the elevation, road width, and slope of main roads. Boyko and Funkhouser (2011) produced a 3D representation of the map by projecting a 2D map onto 3D point clouds. Then, they divided the road network into patches by using the map spline. The location of the curbs in each patch was detected by fitting a 2D active contour to an attractor function. Finally, they labeled the points lying within the active contour as road points.

Since the point cloud data are collected by the vehicle carrying the MLS system driving along the road, the trajectory data and scan line could be obtained by the data acquisition process. Many studies extracted roads with the help of trajectory and scan lines. Kumar et al. (2010) created a set of road cross sections by the point clouds and

navigation data, the cross-sections were processed into 2D lines, and the road edges were extracted from these lines based on the slope, returned intensity, returned pulse width, and proximity to the vehicle. Wang et al. (2012) used the trajectory points as the seed of the searching algorithm to extract the road surface points and detected the boundary of the road by a statistical hypothesis testing method. In their following work, Wang et al. (2015) partitioned the points by trajectory data, and directly constructed a saliency map. Then, the road curbs and boundaries were detected based on the selected characteristics. Cabo et al. (2016) proposed a road asphalt edge delineation algorithm by using the line clouds concept.

The intensity of wavelength is one of the unique characteristics of LiDAR data. Different objects show different reflection intensities. Therefore, the intensity information is popularly used. Teo and Yu (2015) rough recognized the road points by calculating the surface normal vector for each scan line and refined the road surface points by empirical radiometric normalization. Caltagirone et al. (2017) proposed a road detection method by applying FCN. They projected the MLS point clouds from top-view, and generated several feature images, like elevation and density feature images. Then, the FCN was designed for road detection. Lyu et al. (2018) proposed a real-time road segmentation method based on CNNs. They projected the point clouds from Cartesian coordinate into a spherical coordinate and converted the characteristics (like coordinates and intensity) into feature maps as the input of the neural network. Then, a neural network model composed of 11 convolutional layers was used to segment the road surface.

For road geometric shape-based methods, they also can be regarded as the road area extraction and road line extraction methods like we categorized the road extraction methods in section 3.1.1. The methods, which extract road mainly based on the flatness and smoothness, can directly identify the 3D road surface points. Compared with these methods, the other boundary and curb based methods indirectly recognize the road area by detecting or extracting the road edge or boundary, which not only reduce the computational consumption but also obtain the more precise road boundary.

Since the performance of road geometric shape-based methods is heavily limited by the road quality, for example the potholes, cracks, and shelters on the road will noticeable effect the extraction results, data characteristics-based methods can alleviate the problem to some extent. Actually, there are many studies combine these two aspect features to extract the road surface points, especially for the complex scenes.

3.4.2. Road extraction by ALS

Fig. 9 shows the chronological overview of the most relevant methods of road extraction from ALS data. We will review the works on road extraction from ALS data based on their respected publications time.

By virtue of the extraordinary capacity of a wide range of data collection, the airborne LiDAR technique has gained more popularity for road extraction in recent years. Zhao et al. (2011) converted the point clouds into intensity and depth images, and the EM algorithm was used to generate the road candidate image. Then, the road centerline was extracted from the segmented image, and the road intersections were detected by a Radius-Rotating method. Zhao and You (2012) searched the road candidates from the separated ground points by the template fitting, and determined the road widths and orientations by field voting. Li and Lim (2014) partitioned and reordered the road points firstly, and used a moving window classification technique to detect the road points. Hu et al. (2014) used an adaptive mean shift algorithm to detect the road center points based on the filtered ground points and the weighted Hough Transform to extract the arc primitives and grouped them into the road centerline extraction results. Matkan et al. (2014) applied the SVM to extract road, the intensity and range data were used to separate roads from other urban features. Narwade and Musande (2014) utilized Segmentation Based Filtering (SBF) and constrained Delaunay Triangular Irregular Network (CD-TIN) to extract road points. Li et al. (2015) constructed the point cloud topology using a grid index structure and filtered the ground points using a Modified White Top-Hat (MWTH) algorithm. Then, the road candidates were distinguished by local intensity distribution histogram, and the road points were detected by the global inference based on roughness and area. To address the drawbacks of the decision of road intensity threshold based on experience, Hui et al. (2016) extracted the road centerline by hierarchical fusion and optimization. Li et al. (2016c) utilized the elevation and surface roughness to separate roads, and extracted the primitive road centerlines by PCA. Upadhayay et al. (2018) converted the point clouds into intensity and depth image, and generated the classified binary image and DTM mask by the modified maximum likelihood classification algorithm and hierarchical morphology respectively. Then, the classified binary image and DTM mask were integrated to obtain the road candidate image. Truong-Hong et al. (2019) extracted road edges by filtering ground points, extracting and grouping points of road edges, and eliminating incorrect road edge segments. Tejenaki et al. (2019) generated the intensity, DSM, and DTM (digital terrain model) by using LiDAR data, and detected the road surface by Mean Shift segmentation. Previtali et al. (2020) extracted the road network by labelling road points, multi-level voting scheme, and regularization of extracted road segments. To address the issue of manual input of intensity threshold, Sánchez et al. (2020) modified the skewness balancing algorithm to choose the optimal intensity threshold and achieved promising road extraction results on ten study sites. Yadav (2021) combined radiometric, geometric and statistical constraints for road points separation, and extracted road

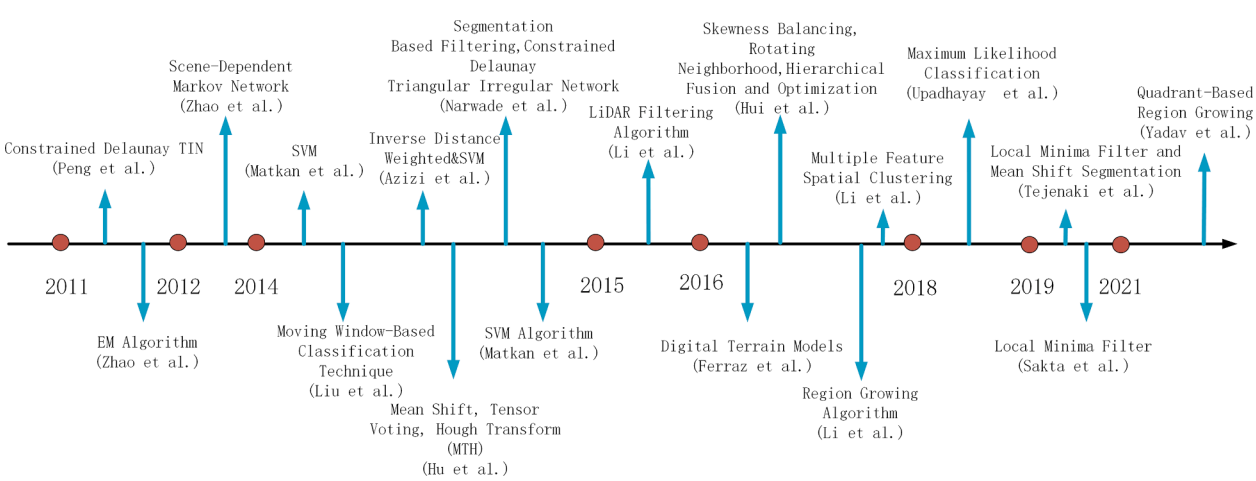

Fig. 9. Chronological overview of our reviewed papers about road extraction from ALS data.

by three steps, intensity-based filtering, quadrant-based region growing, and road candidate regions extraction.

For the road of a specific region, like forest road, many researchers adopt airborne LiDAR data to handle road extraction issues for large-scale scenes. Azizi and Najafi (2014) employed the Inverse Distance Weighted (IDW) method to convert LiDAR data into DSM, DTM, and Digital Non-Terrain Model (DNTM). Then, the LiDAR intensity data and DNTM were classified by SVM, and the road edges were defined in the extracted layers. Ferraz et al. (2016) generated the DTM from LiDAR data, and the maps of slope, roughness and slope gradient were computed from the DTM. Then, a Random Forest classifier was utilized to generate the road mask (road and non-road pixels). An extensive graph was built to propose the largest number of conceivable road candidates based on this mask. Finally, the width and slope of the roads were computed, and the road clusters were extracted by Object-Based Image Analysis (OBIA). Li et al. (2016a) extracted four class features (distance, intensity, Full Width at Half Maximum (FWHM), and back scattering cross-section) by waveform denoising, waveform decomposition, and features extraction. Then, the region growing algorithm was applied to segment the extracted four feature images, and the road detected by merging four segmented images. Prendes et al. (2019) classified the converted slope map and intensity images by pixel-based (Maximum likelihood) and object-oriented (Mean Shift segmentation) classification, respectively. Then, the road centerlines were obtained by a majority filter and other data post-processing. Buján et al. (2021) proposed a hierarchical-hybrid classification tool (HyClass) for forest road detection.

3.4.3. Road extraction from TLS

Compared with the flourishing MLS and ALS-based methods, only a few road extraction methods are based on terrestrial LiDAR data. Husain and Vaishya (2018) proposed a pipeline for the detection of road surface, center line, and boundary lines. In the first phase of the pipeline, they generated the intensity images from LiDAR data, detected the candidate road surface pixels, reconstructed the LiDAR data points by the detected pixels, and performed connected component analysis using Cloud Compare software. In the next phase, the designed vertical grids detected the road surface points. Zheng et al. (2019) projected the LiDAR data onto the XOY plane and rasterized the points into grids, and constructed the decision tree based on five features, including Variance of Point Density (VPD), Variance of Average of Point Distance (VAPD), Variance of Average of Point Height (VAPH), Average of Point Frequency (APF), and Variance of Average of Point Intensity (VAPI). Then, the decision tree was trained to classify the grids, and a minimum bounding rectangle algorithm was applied to obtain the road boundaries. Sha et al. (2022) utilized the k nearest-neighbor search method to obtain the neighborhood information of seed points. Then, the point cloud segments were generated by the iterative weighted least square algorithm and spatial structure judgment. Finally, the supervoxels were updated by the normal vectors.

3.5. Road extraction from 3D&2D remotely sensed data

To compensate for the limitations and insufficiencies of taking the single data source input for road extraction, many researchers try to fuse the different source data to achieve better road extraction performance. In terms of data collection sensors, these 3D&2D data fusion-based road extraction methods could mainly be divided into two branches: the fusion of MLS and camera image and the fusion of ALS and aerial image.

Fig. 10 shows the chronological overview of the most relevant methods of road extraction from MLS&CEMARE and ALS&IMAGE. We will introduce the review work about road extraction from 3D&2D remotely sensed data, mainly according to the chronological overview (Figs. 11–16).

3.5.1. Road extraction from the fusion of MLS and camera image

Xiao et al. (2015) detected road based on CRF. Firstly, they aligned the LiDAR data and the image with cross-calibration, which fuses the data collected from different sensors. Then, a boosted decision tree-based classifier was trained for image and point cloud, respectively, and the classifier's output was treated as the unary potential of the corresponding pixel nodes of the random field. Finally, the fused conditional random field was solved by graph cut. Xiao et al. (2017) extended their previous work (Xiao et al., 2015), they proposed a hybrid CRF model to fuse the data collected from camera and LiDAR. Han et al. (2017) also used CRF to detect road. They also aligned the LiDAR data and the image by cross-calibration as Xiao et al. (2015) did, but replaced the decision tree-based classifier with an Adaboost classifier. Gu et al. (2017) utilized histograms of normalized inverse depths and line scanning to detect road. Gu et al. (2018b) proposed a fully convolutional neural network (FCNN) to detect the road region on the image and a CRF to fuse two road detection results based on their previous work (Gu et al., 2017). The image-based road detection was implemented by FCNN, and the LiDAR-based road detection was implemented by the method proposed in (Gu et al., 2017). Finally, a CRF was used to integrate these two road detection results. To compare the effect of the same road detection method with different data sources, Wulff et al. (2018) proposed the road detection approaches using the fusion of LiDAR and camera data as the input. Firstly, the 15-dimensional occupancy grid maps were calculated by the input LiDAR scan points. Then, the camera images were projected into the Bird-Eye View (BEV) representation and overlaid onto the LiDAR occupancy grid. Thus, the LiDAR and camera data was converted into an 18 channel occupancy grid in BEV. Finally, a modified U-Net FCN was applied to detect the road areas. Li et al. (2021a) also used the BEV of LiDAR data to segment road, but instead of a deep learning-based method. Zhang et al. (2018b) transformed the

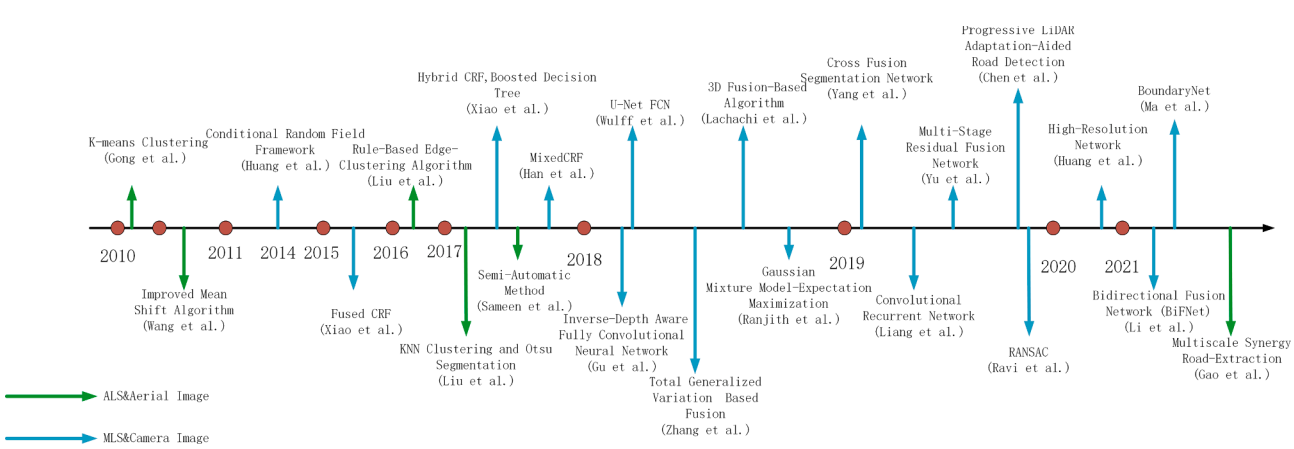

Fig. 10. Chronological overview of our reviewed papers about road extraction from MLS&CEMARE.

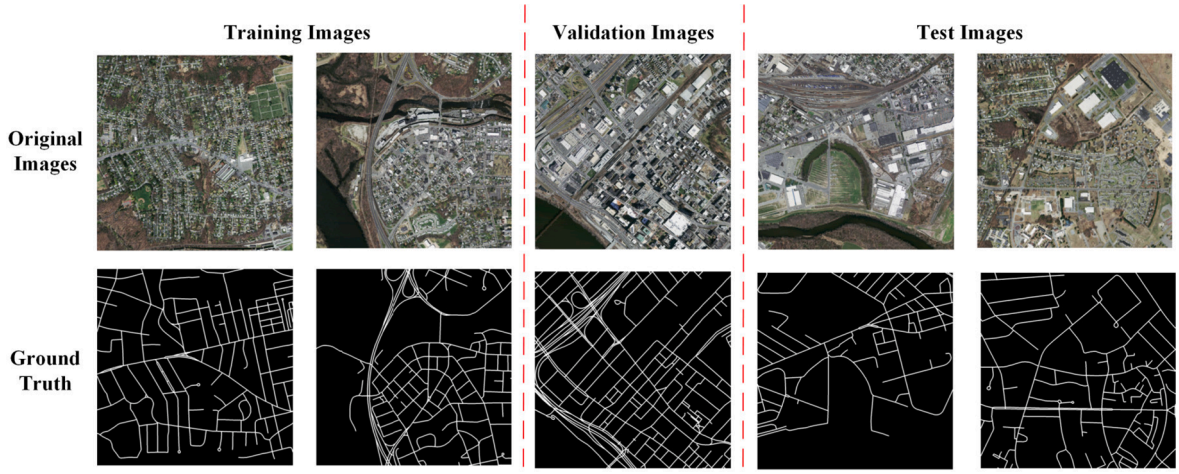

Fig. 11. The exhibition of Massachusetts Road dataset.

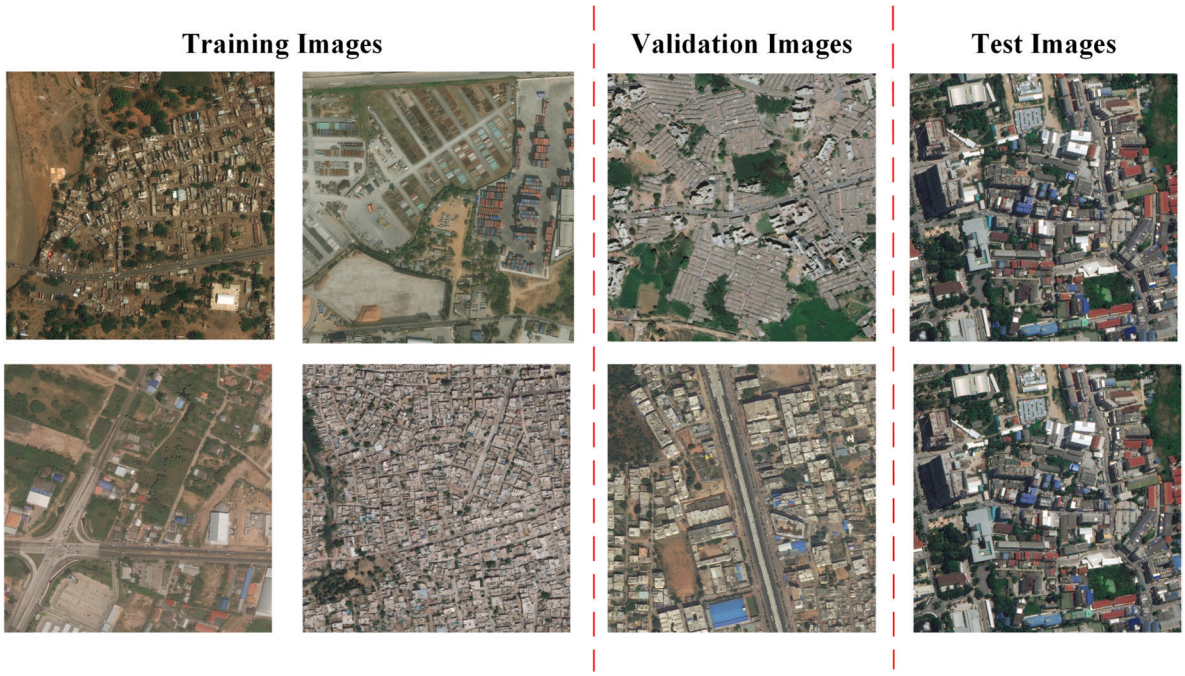

Fig. 12. The exhibition of Deepglobe Road extraction dataset.

point cloud from the spherical coordinate system to the Cartesian coordinate system to obtain a LiDAR imagery, and the flat region was extracted from the LiDAR imagery as the candidate road region. The similar scanning strategy with (Gu et al., 2017) was applied to extract the road region. Finally, they adopted two strategies to fuse the LiDAR-imagering scanning points with an image-guided diffusion. Lachachi et al. (2018) used the stereo camera to guide the road surface extraction from point clouds. Then, the road and sidewalk were separated based on the elevation and illumination invariant colors. Rochan and Sujatha (2018) dynamically extracted the point cloud of free region based on the height difference filter. Then, the filtered point cloud were mapped to the camera image, and the road region was extracted by using Gaussian Mixture Model. Yang et al. (2019a) designed a deep segmentation network to detect road region. The proposed deep segmentation CNN could process both image and point cloud and extract the color features and spatial features. Liang et al. (2019) utilized a FCNN to obtain deep features. Then, a convolutional recurrent network was applied to output the polyline representation of the road boundaries. To overcome the issue of the features extracted from LiDAR and image data do not share the same space, Chen et al. (2019) proposed a progressive LiDAR adaptation road detection method. The data and feature space adaption were implemented via altitude difference-based transformation and cascaded fusion structure respectively. Yu et al. (2019) proposed a FCN-based framework to extract inherent features and merge the feature maps learned from the LiDAR-camera data for road detection. Huang et al. (2020) proposed a road segmentation method based high-resolution network.

3.5.2. *Road extraction from the fusion of ALS and aerial image*

Wang et al. (2011) preprocessed the LiDAR data and aerial images firstly, including the height smooth and data fusion. Then, the fused LiDAR data was classified by using the improved mean-shift algorithm into groups, and the 3D road models were constructed by the classified points and aerial images. Liu and Lim (2016) presented a framework of road extraction. The framework consisted of five main procedures: data fusion, pseudo-scanline creation, initial road extraction, refined road

Fig. 13. The exhibition of LRSNY dataset in (Chen et al., 2021b).

extraction, and final road surface and centerlines extraction. Liu and Lim (2017) did some subtle modifications based on their previous work (Liu and Lim, 2016). Compared with (Liu and Lim, 2016), they did more data pre-processing, like the removal of elevated objects, shadows, and vegetation, and they did not use the pseudo-scanline for road segmentation. Zhang et al., (2018d) extracted the road centerline by road connectivity. Firstly, they did the pre-segmentation of aerial images, and the image segmentations were further classified by the random forest algorithm. Then, to obtain the road network, they proposed a minimum area bounding rectangle (MABR) based filling approach, and adopted the shape filter to construct the road network. Finally, the road centerlines were extracted from the complex road networks. Gao et al. (2021b) proposed a road surface extraction method by multi-scale segmentation and multi-scale feature extraction from aerial images and point cloud rasterized images.

4. Data sets

This section will briefly introduce the commonly used and publicly available data sets for road extraction from 2D, and 3D remotely sensed data.

4.1. 2D remotely sensed datasets

Under our review, there are five commonly used and publicly available 2D data sets for road extraction from remote sensing images, i.e., Massachusetts road dataset(Mnih, 2015), Deepglobe road extraction dataset (Demir et al., 2018), Cheng's road extraction dataset (Cheng et al., 2017), LRSNY dataset (Chen et al., 2021b), and the SpaceNet road dataset (Etten et al., 2018). Table 1 summarizes the features of 5 datasets, after which the details will be introduced.

(1) Massachusetts road dataset.

This dataset is combined with optical remote sensing images, containing 1108 images, 14 images, and 49 images for training, validation and test, respectively. Images in this dataset have a size of 1500 × 1500. The image format is with RGB channels. The resolution of the Massachusetts road dataset is unknown; however, according to our estimation, compared with other known resolution images, we obtain that the resolution of the Massachusetts road dataset is about 1.5 m. The ground truth of each image is a binary image, which uses white color (255,255,255) to denote the road areas and uses color with (0,0,0) to denote the background areas. The applicable road extraction type is cement and asphalt roads. The dataset's URL is: https://www.cs.toronto.edu/~vmnih/data/.

(2) Deepglobe road extraction dataset.

This dataset is a competition dataset used in 2018 Deepglobe road extraction challenge. However, the competition now is closed, and the dataset is unable to download. This dataset contains 6226 training images, 1243 validation images and 1101 test images. Each image has a 1024 × 1024 × 3 size and with a 0.5 m resolution. The images cover areas of Thailand, Indian, and Indonesia. The image format is with RGB channels. The applicable road extraction types contain cement, asphalt and mountain roads. The dataset website can be found in: https://deepglobe.org/challenge.html.

(3) Cheng's road extraction dataset.

The images in this dataset have a spatial resolution of 1.2 m. The size of each image in this dataset is larger than 600 × 600. The labels of this data contain the road areas and the road centerlines. The images are

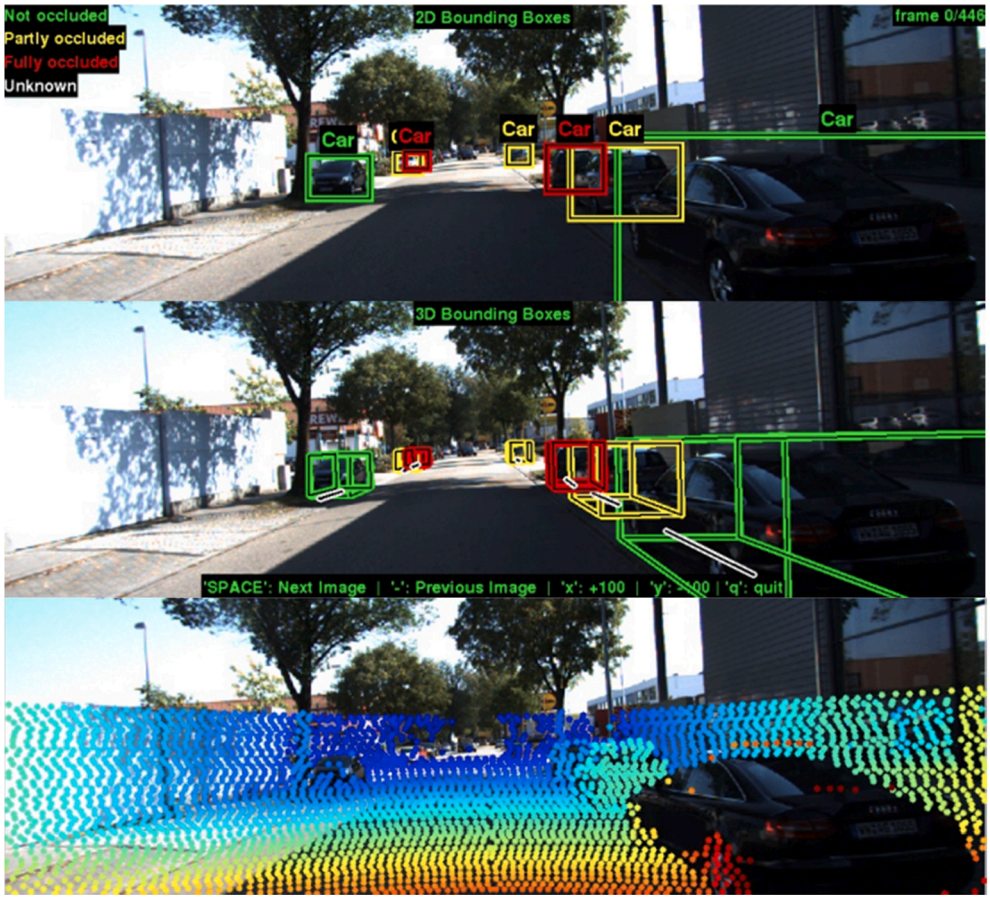

Fig. 14. Examples from the KITTI dataset.

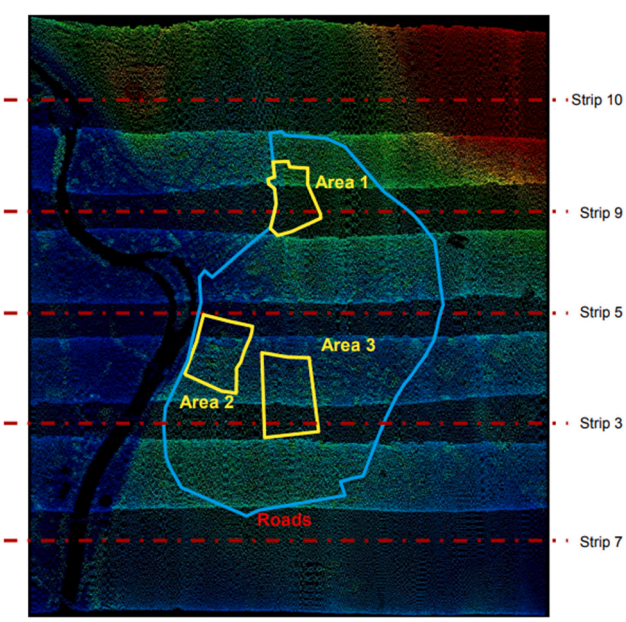

Fig. 15. The ALS data of the Vaihingen dataset.

with RGB format. The applicable road extraction type is cement and asphalt roads. The author informed that the dataset would be publicly available in the future; however, the dataset is still not publicly available.

(4) LRSNY dataset.

This dataset captures the images of the center part of New York City with a resolution of 0.5 m. To make users easily and standardly use the dataset, the original large image is divided into pieces that have a size of 1000 × 1000. The images are with RGB format. The applicable road extraction type is cement and asphalt roads. After the training, validation, and testing separation, it finally generates 716, 220, and 432 images for training, validation, and testing, respectively. Besides the images with a size of 1000 × 1000, this dataset also provides a version of images with a size of 256 × 256. This dataset is publicly available now with the following two websites: https://39.98.109.195:1234/share/Y0fT9h2M and https://pan.baidu.com/s/1jkKPjLYeadRipLGzTNxLgA. During downloading, the users need to fill in the extraction code of "0000" when using the second website. The detailed download information is also located at: https://github.com/zaswczy/LRSNY-dataset/blob/main/Download.

(5) SpaceNet road centerline dataset.

SpaceNet road dataset (Etten et al., 2018) contains VHR images of Las Vegas, Paris, Shanghai and Khartoum with a resolution of 0.3 m, which are captured by WorldView-3. Each image in SpaceNet road dataset has an image size of 3000 × 3000. The image numbers for training, validation and test are 1659, 290 and 568, respectively. The images are with RGB format. The applicable road extraction type is cement and asphalt roads. The major shortcoming of this dataset is that only centerline labels are available. The related website is here: https://registry.opendata.aws/spacenet/.

We know from the above introduction that there are only two publicly available road area extraction datasets, i.e., the Massachusetts road extraction dataset and the LRSNY dataset. Only one publicly available dataset for road centerline extraction from remote sensing images, i.e., SpaceNet road dataset. Right now, there is no publicly available datasets for road extraction from SAR images under our review. There are also

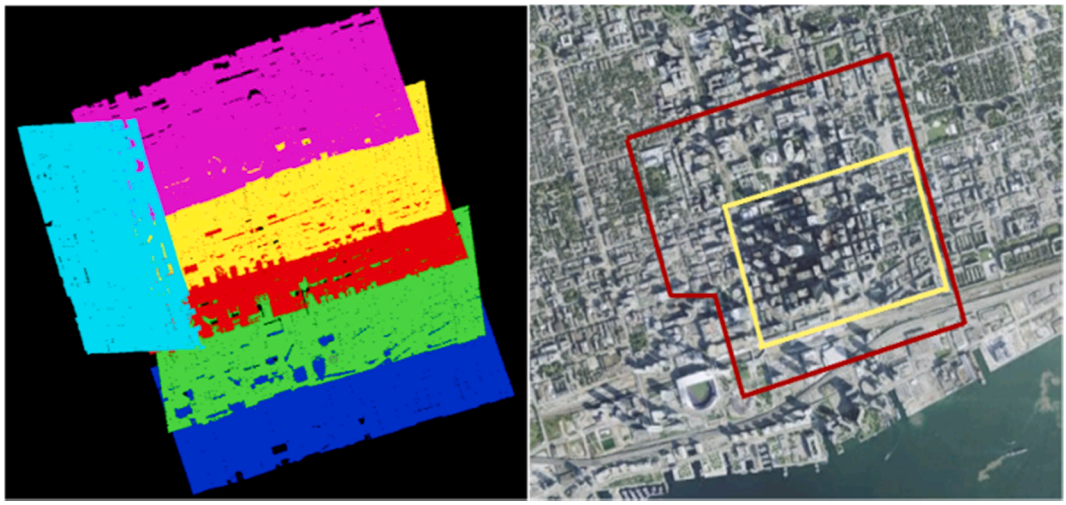

Fig. 16. The ALS data of the Toronto dataset and its coverage.

Table 1
Benchmark datasets for road extraction from 2D remote sensing images.

Dataset/Reference	Sensor	Format	Resolution	Sizes (Each)	Classes	Example Classes
Massachusetts road dataset(Mnih, 2015)	Unknown	RGB	≈1.5 *m*	1500 × 1500	2	Road and Background
Deepglobe road extraction dataset(Demir et al., 2018)	Unknown	RGB	0.5 *m*	1024 × 1024	2	Road and Background
Cheng's road extraction dataset(Cheng et al., 2017)	Unknown	RGB	1.2 *m*	600 × 600	2	Road and Background
LRSNY dataset(Chen et al., 2021b)	Unknown	RGB	0.5 *m*	1000 × 1000	2	Road and Background
SpaceNet road dataset (Etten et al., 2018)	WorldView-3	RGB	0.3 *m*	3000 × 3000	2	Road and Background

existing several datasets which are not standard, or not specially designed or not publicly open for road extraction from remote sensing images, such as GF2 used in (Dai et al., 2020a), NWPUVHR-10 used in (Gao et al., 2021a), etc.

4.2. 3D remotely sensed datasets

Recently, with the development of LiDAR sensor technology, more and more 3D point cloud datasets emerge. But the commonly used and publicly available 3D data sets for road extraction are KITTI and Vaihingen and Toronto datasets (ISPRS). Table 2 summarizes the features of 2 datasets, after which the details will be introduced (see Tables 3–9).

(1) Kitti.

The KITTI dataset (Andreas et al., 2013) is captured from a moving platform while driving in and around Karlsruhe, Germany. The dataset includes camera images, laser scans, high-precision GPS measurements and IMU accelerations from a combined GPS/IMU system. For 3D object detection task, the dataset provides 7481 training images and 7518 test images as well as the corresponding point clouds, comprising a total of 80.256 labeled objects. There are three different road scene categories contained in this dataset, includingurban marked roads (UM), urban multiple marked lanes (UMM), and urban unmarked roads (UU). The dataset can be downloaded by the following website: https://www.cvlibs.net/datasets/kitti/eval_object.php?obj_benchmark=3d.

(2) Vaihingen and Toronto datasets (ISPRS).

The Vaihingen and Toronto datasets (Cramer, 2010) are provided by the ISPRS Test Project on Urban Classification, 3D Building

Table 3
Quantitative performance results tested on the LRSNY dataset.

Method	Recall (%)	Precision (%)	IoU (%)	F1-Score (%)
SegNet(Badrinarayanan et al., 2017)	91.2	93.2	85.6	92.2
PSPNet-50(Zhao et al., 2017)	91.2	94.4	86.5	92.8
Residual U-Net(Zhang et al., 2018c)	90.2	90.9	82.7	90.6
DeepLabV3(Chen et al., 2018a)	90.6	93.2	85.0	91.9
DANet(Fu et al., 2019)	90.5	**94.5**	86.0	92.5
AEML U-Nets(Chen et al., 2021c)	**94.1**	93.4	**88.2**	**93.7**

Table 2
Benchmark datasets for road extraction from 3D point clouds.

Dataset	Sensor	Format	Primary Fields	Sizes	Classes	Example Classes
KITTI	Velodyne HDL-64E	bin	X, Y, Z Intensity Class	29 GB	9	car, van, truck, pedestrian…
Vaihingen (ISPRS)	Leica ALS50	las	X, Y, Z Intensity Class	552 MB	9	powerline, low vegetation, impervious surface, fence/hedge, car, roof, facade, shrub, tree
Toronto (ISPRS)	ALTM-ORION M	las	X, Y, Z Intensity Class	370 MB	9	powerline, low vegetation, impervious surface, fence/hedge, car, roof, facade, shrub, tree

Table 4
The quantitative performance results tested on the Massachusetts road dataset.

Method	Recall (%)	Precision (%)	IoU (%)	F1-Score (%)
SegNet (Badrinarayanan et al., 2017)	72.1	82.5	62.5	76.9
PSPNet-50 (Zhao et al., 2017)	76.3	77.9	62.7	77.1
Residual U-Net (Zhang et al., 2018c)	79.7	76.9	64.3	78.3
DeepLabV3 (Chen et al., 2018c)	74.0	78.3	61.4	76.1
DANet (Fu et al., 2019)	74.2	81.2	63.3	77.6
AEML U-Nets(Chen et al., 2021c)	76.3	81.1	64.8	78.6
RDRCNN (Gao et al., 2019)	75.3	84.6	66.3	79.7
RDRCNN + postprocess (Gao et al., 2019)	75.8	85.4	67.1	80.3
MsGAN (Zhang et al., 2019b)	87.1	85.3	–	86.2
DiResNet (Ding and Bruzzone, 2020)	80.3	80.1	60.7	80.1
SSLF (Guo and Wang, 2020)	42.0	34.6	22.6	–
DW-CNN (Lian and Huang, 2020)	82.7	82.3	–	82.5
CNN-BS&T (Wei et al., 2020)	85.9	78.5	**78.7(buffer)**	–
ICIE-DNet (Wang et al., 2021b)	82.2	87.1	–	84.6
ELU-SegNet(Panboonyuen et al., 2017)	73.3	85.2	–	78.8
ELU-SegNet-LMs(Panboonyuen et al., 2017)	86.1	85.4	–	85.7
ELU-SegNet-LMs-CRFs(Panboonyuen et al., 2017)	89.4	85.8	–	87.6
ASPP-U-net(He et al., 2019)	81.9	84.9	–	83.2
ASPP-U-net-SSIM (He et al., 2019)	80.5	87.1	–	83.5
PP&CNN (Manandhar et al., 2019)	90.8	**94.4**	–	–
DenseUNet (Xin et al., 2019)	70.4	78.3	74.5(mIoU)	74.1
JointNet (Zhang and Wang, 2019)	71.9	85.4	64.0	–
D-EDTNet (Geng et al., 2020)	79.4	69.9	59.2	74.2
DAD-LinkNet (Gao et al., 2021a)	78.9	84.3	67.7	78.1
RDNNs (Li et al., 2021c)	91.0	85.0	–	**87.9**
SRG(Cui et al., 2021)	**93.6**	67.6	62.2	–
SGCN(Zhou et al., 2022)	73.9	84.8	65.3	79.0
DCS-TransUperNet(Zhang et al., 2022)	78.4	82.4	65.4	80.4
UNet(Ronneberger et al., 2015)	70.4	82.3	61.1	75.9
UNet++(Zhou et al., 2018)	72.4	80.9	61.8	76.4
Attention UNet(Oktay et al., 2018)	68.4	83.0	60.0	75.0
FCNs(Long et al., 2017)	68.1	82.8	59.7	74.7
CADUNet(Li et al., 2021b)	76.6	79.5	64.1	77.9
GAE-LinkNet(Li et al., 2021e)	68.7	80.5	58.9	74.2
Batra(Batra et al., 2019)	69.3	81.9	60.1	75.1

Reconstruction and Semantic Labeling. These two datasets can be downloaded by the following website:https://www.isprs.org/education/benchmarks/UrbanSemLab/Default.aspx.

The Vaihingen dataset provides the airborne laser scanning data from the city of Vaihingen, Germany. The dataset collects the point clouds by a Leica ALS50 ALS system, and the point density is 4 points/m^2. There are nine classes objects included in this dataset. The dataset contains three different scenes, the biggest one has 753,876 points as the training scene, and the other two smaller scenes has total 411,722 points as the test scenes.

The Toronto dataset provides the airborne laser scanning data from the city of Toronto, Canada. The dataset acquired by Optech's ALTM-ORION M, and the point density is approximately 6 points/m^2. The labeled classes of objects is the same as Vaihingen dataset. The dataset contains one whole scene, Downtown Toronto, and its two sub-scene.

Table 5
Quantitative performance results tested on the Cheng's road extraction dataset.

Method	Recall (%)	Precision (%)	IoU (%)	F1-Score (%)
RDNNs (Li et al., 2021c)	87.4	88.1	–	87.8
MF&M−NMS (Cheng et al., 2016a)	94.3	89.5	84.9	–
GL-Dense-U-Net (Xu et al., 2018)	95.2	96.3	–	95.7
AMSMT-UNet (Lu et al., 2019)	95.9	95.5	91.8	–
AMT-UNet (Lu et al., 2019)	94.9	94.8	90.2	–
RCNN-UNet (Yang et al., 2019b)	**97.7**	96.9	**93.6**	**97.3**
MsGAN (Zhang et al., 2019b)	96.0	**97.4**	–	96.7
ScRoadExtractor (Wei and Ji, 2020)	84.2	90.3	76.5	86.6

Table 6
Quantitative performance results tested on the GF-2 road dataset.

Method	Recall (%)	Precision (%)	IoU (%)	F1-Score (%)
RDRCNN (Gao et al., 2019)	80.9	80.9	64.2	78.2
RDRCNN + Postprocess (Gao et al., 2019)	80.1	82.4	**64.7**	**78.6**
MLSOH (Dai et al., 2020a)	**98.7**	**99.5**	–	–
MRENet (Shao et al., 2021)	67.7	75.5	55.5	71.4

Table 7
The quantitative performance results tested on the Deepglobe road extraction dataset.

Method	Recall (%)	Precision (%)	IoU (%)	F1-Score (%)
GOALF (Lu et al., 2021b)	70.8	73.2	56.2	72.0
GCB-Net (Zhu et al., 2021)	–	–	**70.8**	**81.5**
DiResNet (Ding and Bruzzone, 2020)	**81.5**	78.8	66.8	79.1
ScRoadExtractor (Wei and Ji, 2020)	71.4	**79.5**	57.8	71.3
DCS-TransUperNet(Zhang et al., 2022)	69.5	77.9	56.7	73.5

Table 8
Quantitative performance results tested on the SpaceNet road extraction dataset.

Method	Recall (%)	Precision (%)	IoU (%)	F1-Score (%)
GCB-Net (Zhu et al., 2021)	–	–	**69.1**	**76.3**
GOALF (Lu et al., 2021b)	**68.9**	**64.2**	49.8	66.5

5. Performance review

In this section, we first introduce the commonly used evaluation

Table 9
Quantitative performance results of MLS.

Method	Recall (%)	Precision (%)	IoU (%)	Dataset
RG-BF&S-BR(Yadav et al., 2017)	95.6	97.9	93.7	Self-collected
MWO (Yang et al., 2013)	95.1	98.1	93.4	Self-collected
MO (RodrguezCuenca, 2015)	97.7	98.3	**96.1**	Self-collected
PCA-P-BM(Wang et al., 2015)	95.4	99.4	94.8	Self-collected
LCPM (Xu et al., 2017b)	78.6	83.3	–	Self-collected
SW(Cabo et al., 2016)	97	99	–	Self-collected
HD&TNRG(Miraliakbari et al., 2015)	93.8	94.9	–	Self-collected
GVF&BPACM(Kumar et al., 2013)	98.5	**100**	–	Self-collected
FPGA-CNN(Lyu et al., 2018)	–	84.8	–	KITTI
D-DA(Teo and Yu, 2015)	95.6	98.7	–	Self-collected
CED(El-Halawany et al., 2011)	94	97	–	Self-collected
CEC(Ma et al., 2019)	90.8	93.9	–	Self-collected
M−RRGM (Yang et al., 2017a)	91.2	90.6	–	Self-collected
BKD(Yang et al., 2017b)	98.4	95.4	–	Self-collected
LM& RANSAC (Gu et al., 2018a)	92.0	98.0	–	Self-collected
RANSAC(Qiu et al., 2016)	97.3	99.9	–	Self-collected
α-SA (Zai et al., 2018)	96.6	98.5	95.2	Self-collected
PG-BM(Sun et al., 2019a)	95.9	95.0	–	Self-collected
IDW (Guan et al., 2014)	96	83	–	Self-collected
ITV (Guan et al., 2015)	96	93	–	Self-collected
RWF (Guo et al., 2015)	96.4	98.7	95.1	Self-collected
T-SM (Yadav and Singh, 2017)	94.2	96.3	90.9	Self-collected
SGM(Mi et al., 2021)	92.1	95.3	–	Self-collected
M−FL−TM(Wang et al., 2021a)	86.2	90.0	–	KITTI
DBSCAN (Jung et al., 2020)	93.1	90.1	–	Self-collected
ATSM (Huang et al., 2021)	87.4	94.5	–	Self-collected
RBNN-CA (Zhao et al., 2021)	**99.8**	99.7	–	Self-collected
S-BM(Zhang et al., 2018a)	82.9	84.9	–	Self-collected

metrics in road extraction from remote sensing data, including 2D and 3D data. Then, we show the quantitative performances of related works with evaluation metrics for the readers.

5.1. Evaluation metrics

(1) 2D remote sensing images

In road extraction from 2D remote sensing images, the commonly used performance evaluation method contain four metrics: i.e., Recall, Precision, IoU, and F1-Score.

The representations of the four metrics are as follows:

$$\text{Reccall} = \frac{TP}{TP + FN}, \tag{1}$$

$$\text{Precision} = \frac{TP}{TP + FP}, \tag{2}$$

$$\text{IoU} = \frac{TP}{TP + FN + FP}, \tag{3}$$

$$F1 - Score = \frac{2*Precision*Recall}{Precision + Recall}, \tag{4}$$

where TP, FN and FP are the true positive, false negative and false positive, respectively.

(2) 3D.

Except the metrics for 2D, the Completeness, Correctness, and Quality metrics are widely used for road extraction from 3D remote sensing data. The metrics are defined as follows:

$$Completeness = \frac{TP}{L_r}, \tag{5}$$

$$Correctness = \frac{TP}{L_e}, \tag{6}$$

$$Quality = \frac{TP}{L_e + FN}, \tag{7}$$

where L_r is the total length of the reference road, L_e is the total length of extracted road. It should be note that the "Completeness", "Correctness" and "Quality" are equal to "Recall", "Precision" and "IoU", respectively. To make table headers in 3D be consistent with that in 2D, we use the "Recall", "Precision" and "IoU" as table headers in the following performance tables of 3D.

5.2. Quantitative performance (2D, 3D)

(1) In 2D remote sensing datasets.

For LRSNY dataset, the best IoU score under our review is obtained by (Chen et al., 2021c), which is 88.2%. For Massachusetts dataset, there are 29 approaches' test results in Table 4, among which (Wei et al., 2020) achieved the best IoU score (78.7%). Note that, Wei et al. (2020) tested their model with a 4 pixels buffer, while most methods did not. Besides, Xin et al. (2019) obtained a IoU score higher than 70% due to using average IoU. For the Deepgloble dataset, the best performance is as high as 70.8% IoU score within our reviewed papers.

(2) In 3D remote sensing datasets.

Since the most of methods mentioned in section 3.2 extract the roads by the self-collected dataset, it is hard to compare these methods based on the results of accuracies. For Vaihingen and Toronto datasets (ISPRS), the recent study (Tejenaki, 2019) does the comprehensive comparison with the previous methods, and achieve better road extraction performance by focusing on the road connectivity and continuity.

(3) In 3D&2D remote sensing datasets.

By virtue of data comprehensiveness, the KITTI dataset provides both camera images and the corresponding point clouds, which is naturally suitable for the fusion of 3D and 2D data. Thus, most of the methods mentioned in section 3.3.1 extract roads on KITTI dataset. As show in Table 10, (Chen et al., 2019) and (Huang et al., 2020) achieves high precision and recall on KITTI dataset, which mainly due to the use of deep learning methods and the more comprehensive features (see Tables 11 and 12).

6. Discussion

6.1. Observed trends

(1)Observed Trends in Road Extraction from 2D Remote Sensing Images.

First, the optical remote sensing images are more preferred

Table 10
Quantitative performance results of ALS.

Method	Recall (%)	Precision (%)	IoU (%)	Dataset
EMA (Zhao et al., 2011)	93	93	–	Self-collected
S-DMN(Zhao and You, 2012)	91.8	89.2	82.6	Self-collected
MW-BCT (Li and Lim, 2014)	92.0	**96.0**	**91.6**	Self-collected
IDW&SVM(Azizi and Najafi, 2014)	75.1	63.0	52.1	Self-collected
MTH(Hu et al., 2014)	53.4	73.8	44.9	Vaihingen dataset(ISPRS)
SBF& CD-TIN (Narwade and Musande, 2014)	83.4	83.0	83.2	Vaihingen dataset(ISPRS)
SRH (Hui et al., 2016)	80.4	91.4	74.8	Vaihingen dataset(ISPRS)
LMF&MSS(Tejenaki et al., 2019)	95.9	83.7	80.8	Vaihingen dataset(ISPRS)
LFA (Li et al., 2015)	93	76	–	Self-collected
SVMc&RM (Matkan et al., 2014)	**96.4**	93.3	90.1	Self-collected

Table 11
Quantitative performance results of TLS.

Method	Recall (%)	Precision (%)	IoU (%)	Dataset
Husain et al. 2018 (Husain and Vaishya, 2018)	**93.9**	**96.9**	–	Self-collected

Table 12
Quantitative performance results of 3D&2D remote sensing data.

Method	Recall (%)	Precision (%)	IoU (%)	Dataset
R-BE-CA (Liu and Lim, 2016)	89.2	91.2	88.1	Self-collected
OS&HMF&KNNC (Liu and Lim, 2017)	82.9	84.1	83.2	Self-collected
FCRF(Xiao et al., 2015)	93.4	83.6	–	KITTI
HCRF (Xiao et al., 2017)	91.3	90.7	–	KITTI
RANSAC &ICP(Gu et al., 2018a)	92.0	**98.0**	–	Self-collected
UG-F (Wulff et al., 2018)	93.9	93.7	–	KITTI
IDA-FCNN (Gu et al., 2018b)	96.1	96.7	–	KITTI
S + TGV (Zhang et al., 2018b)	95.7	96.5	–	KITTI
3D-FBA (Lachachi et al., 2018)	**98.2**	82.8	–	KITTI
CFSN (Yang et al., 2019a)	86.1	81.2	–	KITTI
CRN (Liang et al., 2019)	94.6	94.8	–	Self-collected
PLARD (Chen et al., 2019)	96.9	97.2	–	KITTI
H-RN (Huang et al., 2020)	92.0	91.6	–	KITTI
MixedCRF (Han et al., 2017)	93.2	90.0	–	KITTI
BiFNet (Li et al., 2021a)	95.4	95.5	–	KITTI
M−SRFN (Yu et al., 2019)	95.1	96.9	–	KITTI
c-DCGAN (Ma et al., 2021)	92.2	96.1	88.9	Self-collected
MSRE (Gao et al., 2021b)	97.8	93.7	**91.7**	Self-collected

compared to the SAR images. Under this review, the related works about road extractions from 2D optical remote sensing images are about 3 times more than the related road extraction works from 2D SAR images. Although SAR images now can provide images with resolution as high as optical remote sensing images, the optical remote sensing images still present much more color and texture information during road extraction. On the other hand, the SAR images also have the advantages of working conditions, i.e., the SAR images can work on the whole day under all weather conditions. In contrast, the optical remote sensing images are failed to collect at night and under cloudy weather.

Second, deep learning-based methods illustrate more and more power and effectiveness. In the latest 5 years, deep learning-based methods have dominated the road extraction from 2D remote sensing images. On the other hand, traditional methods that use handcrafted features and morphological features are almost neglected. Usually, the handcrafted features and morphological feature-based methods can be used as post-processing approach to promote the accuracy of deep learning-based results.

Third, the datasets play a more important role in road extraction from 2D remotely sensed images since the fast development of deep learning-based methods. Unlike handcrafted features based and morphological features based approaches, the deep learning-based algorithms need a large enough dataset with accurate labels to train a deep learning model, leading to hard burdens of manually labeling works.

(2) Observed Trends in Road Extraction from 3D Point Clouds.

First, in terms of data, the MLS data natively has higher point density and precision than ALS data and TLS data for road extraction. Thus, the number of articles based on MLS data for road extraction is the largest. For some special road, such as the forest road, the mobile platforms are difficult to operate there, the ALS data or TLS data are more suitable to this situation. Except the point density and precision, the recent studies are also enthusiastic about using more information contained and 3D&2D integrated data. Fortunately, some datasets, like KITTI, provide information captured by various sensors including visual cameras, LiDAR sensor, and GPS, which is convenient for the related researches.

Second, in terms of method, compared with the early methods, which choose some geometric shape characteristics of road and set the corresponding thresholds to filter the road points, the follow-up studies consider the more comprehensive features of road and powerful classifiers to achieve better extraction performance. Naturally, with the improvement of the techniques of feature extraction and feature representation, the automation of road extraction has increased accordingly. In recent years, the deep learning-based methods are gradually applied into object extraction from 3D point clouds, which provide the more powerful classification ability than the traditional machine learning classifiers.

6.2. Challenges and future trends

(1) Challenges and future trends in road extraction from 2D remote sensing images.

First, the performance of road extraction from 2D remote sensing images can still be improved. Although the performance of road extraction from 2D remote sensing images has achieved great progress since the applications of deep learning methods, the extraction results still suffer from the errors caused by shadows, occlusions, interferences of similar background areas, etc. In our opinion, two strategies may be used to conquer the above problems in the future. The first strategy is to fuse the optical and SAR images. The SAR and optical images have quite different properties and advantages, which may complement each other. On the other hand, research regarding the fusion of optical and SAR images are limited. The second strategy is to fuse traditional features and deep learning features for road extraction from 2D remote sensing images. At present, the combination of traditional and deep learning features stays at low-level, which simply combines two kinds of features as pipeline processing. In fact, embedding the traditional features into a deep learning framework with an end-to-end training format has a great value for research. The related research is still insufficient.

Second, the context information quarrying and utilizing is still insufficient as the road extraction results still have many limitations. The multi-scale convolution kernels have been widely used to enhance the context information learning ability. However, the exploration of the context among objects has rarely been studied, which is important for human cognitive ability to implement. Thus, the research using the relationship among different objects may be a breakthrough for road

extraction from remote sensing images.

Third, the accurately labeled data sets are still insufficient and in need urgently. Under our review, there are only two publicly available datasets specially designed for road extraction from remote sensing images. However, deep learning-based research needs a large amount of accurately labeled data sets for its supports. Thus, producing large, well-labeled datasets is meaningful and will have chances in the future.

Fourth, how to enhance the extensibility of the road extraction models is still a challenging problem that needs to be further studied. The present models are usually specially designed or trained for special datasets under given resolution and images characteristics. When applied the trained model to another dataset, a large work about model retraining and re-adjusting is needed. How to reduce the cost of model transplantation is still needs to be studied in the future, which may be a good opportunity for researchers.

(2) Challenges and future trends in road extraction from 3D point clouds.

First, most of the existing studies only focus on the small regions of road sections; there are few methods designed for the large-scale scenes' road extraction. For large-scale scenes, the total volumes of point cloud data will increase dramatically as the area increase. How to handle the massive point cloud data with limited computational and storage resources is still a challenge. Some deep learning methods have recently been proposed for large-scale point cloud processing, that are the hope for the next generation challenges. However, accurate labelling for large data is still a challenge and far way to go.

Second, the automation of road extraction still needs to be improved. Although the latest methods are more automated than a decade ago, it is still difficult to achieve the full automation of road extraction. For unsupervised methods, hand craft feature extraction or data preprocessing is still necessary in many cases. For supervised methods, manually labeling training data is an inevitable extra preparatory work.

Third, the high accuracy and high-resolution road extraction result are still difficult to obtain. Unlike the road extraction from 2D images, due to the unstructured and irregular properties of point cloud data, with unavoidable presence of noise, occlusions and outliers, it is difficult to achieve the high accuracy road extraction results from 3D point clouds. As to the rasterization or voxelization processing, that will inevitably reduce the resolution of road extraction results.

7. Conclusion

This paper presents a detailed review of road extraction from remote sensing data in the last 10 years, introducing more than 240 papers in total. We first show the general overviews of road extractions from both 2D remote sensing images and 3D point clouds. Then, we give detailed reviews from 2D and 3D perspectives, respectively. In 2D perspective, we illustrated in detail about works using two kinds of commonly used images, i.e., optical and SAR image. More than 120 papers were covered in that section, among which we has a bias focusing on the deep learning approaches. In 3D perspective, road extraction by MLS, ALS, and TLS were introduced, respectively. For 3D methods, more than 90 papers were reviewed. We also gave an investigation about the 3D&2D road extraction approaches. After reviewing methodologies, we also give a detailed introduction about the datasets in road extraction from both 2D remote sensing images and 3D point clouds, including 5 datasets and 2 datasets for 2D and 3D, respectively. To make the readers be clear about the performances of the existing popular methods, the performances comparisons according to the reported results were met and shown. Finally, we presented the observed trends, challenges, and future opportunities about road extraction from remotely sensed data. From our review, the data fusion, context information learning, and data sets construction etc., may be the trends and opportunities for future researches studying road extraction from remotely sensed data.

Funding

This study was financially supported by National Natural Science Foundation of China (No.62001175), in part by the Fundamental Research Funds for the Central Universities of Huaqiao University (No. ZQN-911), in part by the Natural Science Foundation of Fujian Province (No. 2021 J05059), in part by the Open Research Fund of State Key Laboratory of Information Engineering in Surveying, Mapping and Remote Sensing, Wuhan University (No.21E01), in part by the Scientific Research Funds of Huaqiao University (NO. 605-50Y21026), in part by the National Natural Science Foundation of China (No.61801121, 41971414 and 62076107) and CAPES PrInt (No. 88881.311850/2018-01).

CRediT authorship contribution statement

Ziyi Chen: Conceptualization, Methodology, Formal analysis, Investigation, Resources, Data curation, Writing – original draft, Writing – review & editing, Visualization, Project administration, Funding acquisition. **Liai Deng:** Data curation, Writing – original draft, Visualization. **Yuhua Luo:** Writing – original draft, Writing – review & editing. **Dilong Li:** Formal analysis, Investigation, Writing – original draft, Visualization. **José Marcato Junior:** Writing – review & editing, Funding acquisition. **Wesley Nunes Gonçalves:** Writing – review & editing, Funding acquisition. **Abdul Awal Md Nurunnabi:** Writing – review & editing. **Jonathan Li:** Conceptualization, Writing – review & editing. **Cheng Wang:** Conceptualization, Supervision, Funding acquisition. **Deren Li:** Methodology, Formal analysis, Data curation, Writing – review & editing, Supervision.

Declaration of Competing Interest

The authors declare that they have no known competing financial interests or personal relationships that could have appeared to influence the work reported in this paper.

References

Alshehhi, R., Marpu, P.R., 2017. Hierarchical graph-based segmentation for extracting road networks from high-resolution satellite images. ISPRS J. Photogramm. Remote Sens. 126, 245–260. https://doi.org/10.1016/J.ISPRSJPRS.2017.02.008.

Alshehhi, R., Marpu, P.R., Wei, L.W., Mura, M.D., 2017. Simultaneous extraction of roads and buildings in remote sensing imagery with convolutional neural networks. ISPRS J. Photogramm. Remote Sens. 130, 139–149. https://doi.org/10.1016/J.ISPRSJPRS.2017.05.002.

Andreas, G., Philip, L., Stiller, C., Urtasun, R., 2013. Vision meets robotics: the kitti dataset. Int. J. Robot. Res. 32 (11), 1231–1237.

Azizi, Z., Najafi, A., 2014. Forest road detection using lidar data. J. For. Res. 25 (4), 975–980.

Badrinarayanan, V., Kendall, A., Cipolla, R., Dec 2017. Segnet: a deep convolutional encoder-decoder architecture for image segmentation. IEEE Trans. Pattern Anal. Mach. Intell. 39 (12), 2481–2495. https://doi.org/10.1109/TPAMI.2016.2644615.

Bae, Y., Lee, W.-H., Choi, Y.-J., Jeon, Y.W., Ra, J., 2015. Automatic road extraction from remote sensing images based on a normalized second derivative map. IEEE Geosci. Remote Sens. Lett. 12, 1858–1862. https://doi.org/10.1109/LGRS.2015.2431268.

Bakhtiari, H.R.R., Abdollahi, A., Rezaeian, H., 2017. Semi automatic road extraction from digital images. Egypt. J. Remote Sens. Space Sci. 20, 117–123. https://doi.org/10.1016/J.EJRS.2017.03.001.

Bastani F., He S., Abbar S., Alizadeh M., and Balakrishnan H., 2018. Roadtracer: Automatic Extraction of Road Networks from Aerial Images. In: Paper presented at the 2018 IEEE/CVF Conference on Computer Vision and Pattern Recognition, Salt Lake City, UT, USA, 18-23 June 2018. 10.1109/CVPR.2018.00496.

Batra A., Singh S., Pang G., Basu S., Jawahar C. V., and Paluri M., 2019. Improved Road Connectivity by Joint Learning of Orientation and Segmentation. In: Paper presented at the 2019 IEEE/CVF Conference on Computer Vision and Pattern Recognition (CVPR), Long Beach, CA, USA, 15-20 June 2019. 10.1109/CVPR.2019.01063.

Boyko, A., Funkhouser, T., 2011. Extracting roads from dense point clouds in large scale urban environment. ISPRS J. Photogramm. Remote Sens. 66, 2–12. https://doi.org/10.1016/J.ISPRSJPRS.2011.09.009.

Buján, S., Guerra-Hernández, J., González-Ferreiro, E., Miranda, D., 2021. Forest road detection using lidar data and hybrid classification. Remote Sensing 13 (3), 393. https://doi.org/10.3390/rs13030393.

Cabo, C., Kukko, A., García-Cortés, S., Kaartinen, H., Hyyppä, J., Ordoñez, C., 2016. An algorithm for automatic road asphalt edge delineation from mobile laser scanner

data using the line clouds concept. Remote Sensing 8 (9), 1–20. https://doi.org/10.3390/RS8090740.

Caltagirone L., Scheidegger S., Svensson L., and Wahde M. 2017. "Fast Lidar-Based Road Detection Using Fully Convolutional Neural Networks," Paper presented at the 2017 IEEE Intelligent Vehicles Symposium (IV), Los Angeles, CA, USA, July 11, 2017. 10.1109/IVS.2017.7995848.

Chaudhuri, D., Kushwaha, N.K., Samal, A., 2012. Semi-automated road detection from high resolution satellite images by directional morphological enhancement and segmentation techniques. IEEE J. Sel. Top. Appl. Earth Obs. Remote Sens. 5 (5), 1538–1544. https://doi.org/10.1109/JSTARS.2012.2199085.

Chen, D., Zhong, Y., Zheng, Z., Ma, A., Lu, X., 2021a. Urban road mapping based on an end-to-end road vectorization mapping network framework. ISPRS J. Photogramm. Remote Sens. 178, 345–365.

Chen, L.-C., Papandreou, G., Kokkinos, I., Murphy, K., Yuille, A., 2018a. Deeplab: semantic image segmentation with deep convolutional nets, atrous convolution, and fully connected Crfs. IEEE Trans. Pattern Anal. Mach. Intell. 40, 834–848. https://doi.org/10.1109/TPAMI.2017.2699184.

Chen, L., Zhu, Q., Xie, X., Hu, H., Zeng, H., 2018b. Road extraction from Vhr remote-sensing imagery via object segmentation constrained by gabor features. ISPRS Int. J. Geo-Inf. 7 (9), 362. https://doi.org/10.3390/ijgi7090362.

Chen, L.C., Papandreou, G., Kokkinos, I., Murphy, K., Yuille, A.L., 2018c. Deeplab: semantic image segmentation with deep convolutional nets, atrous convolution, and fully connected Crfs. IEEE Trans. Patt. Anal. Mach. Intell. 40 (4), 834–848. https://doi.org/10.1109/TPAMI.2017.2699184.

Chen, W., Ouyang, S., Tong, W., Li, X., Zheng, X., Wang, L., 2022. Gcsanet: a global context spatial attention deep learning network for remote sensing scene classification. IEEE J. Sel. Top. Appl. Earth Obs. Remote Sens. 15, 1150–1162. https://doi.org/10.1109/jstars.2022.3141826.

Chen, Z., Zhang, J., Tao, D., 2019. Progressive lidar adaptation for road detection. IEEE/CAA J. Autom. Sin. 006 (003), 693–702. https://doi.org/10.1109/JAS.2019.1911459.

Chen, Z., Wang, C., Li, J., Xie, N., Han, Y., Du, J.-X., 2021b. Reconstruction bias U-net for road extraction from optical remote sensing images. IEEE J. Sel. Top. Appl. Earth Obs. Remote Sens. 14, 2284–2294. https://doi.org/10.1109/JSTARS.2021.3053603.

Chen, Z., Fan, W., Zhong, B., Li, J., Du, J., Wang, C., 2020. Corse-to-fine road extraction based on local dirichlet mixture models and multiscale-high-order deep learning. IEEE Trans. Intell. Transp. Syst. 21, 4283–4293. https://doi.org/10.1109/TITS.2019.2939536.

Chen, Z., Wang, C., Li, J., Fan, W., Du, J., Zhong, B., 2021c. Adaboost-like end-to-end multiple lightweight U-nets for road extraction from optical remote sensing images. Int. J. Appl. Earth Observ. Geoinform. 100, 102341 https://doi.org/10.1016/j.jag.2021.102341.

Cheng, G., Zhu, F., Xiang, S., Pan, C., 2016a. Road centerline extraction via semisupervised segmentation and multidirection nonmaximum suppression. IEEE Geosci. Remote Sens. Lett. 13 (4), 545–549. https://doi.org/10.1109/LGRS.2016.2524025.

Cheng, G., Zhu, F., Xiang, S., Wang, Y., Pan, C., 2016b. Accurate urban road centerline extraction from vhr imagery via multiscale segmentation and tensor voting. Neurocomputing vol. 205, no. C, 407–420. https://doi.org/10.1016/j.neucom.2016.04.026.

Cheng, G., Wang, Y., Xu, S., Wang, H., Xiang, S., Pan, C., 2017. Automatic road detection and centerline extraction via cascaded end-to-end convolutional neural network. IEEE Trans. Geosci. Remote Sens. 55 (6), 3322–3337. https://doi.org/10.1109/TGRS.2017.2669341.

Cheng, J., Ding, W., Ku, X., Sun, J., 2012. Road extraction from high-resolution sar images via automatic local detecting and human-guided global tracking. Int. J. Antennas Propagat. 2012, 1–10. https://doi.org/10.1155/2012/989823.

Cheng, J., Guan, Y., Ku, X., Sun, J., 2011. Semi-Automatic Road Centerline Extraction in High-Resolution Sar Images Based on Circular Template Matching. In: Paper presented at the 2011 International Conference on Electric Information and Control Engineering, Wuhan, China, 15-17 April 2011. 10.1109/ICEICE.2011.5777358.

Cheng, J., Gao, G., 2016. Parallel particle filter for tracking road centrelines from high-resolution sar images using detected road junctions as initial seed points. Int. J. Remote Sens. 37 (20), 4979–5000. https://doi.org/10.1080/01431161.2016.122517.

Cira, C.-I., Alcarria, R., Manso-Callejo, M.-Á., Serradilla, F., 2020. A framework based on nesting of convolutional neural networks to classify secondary roads in high resolution aerial orthoimages. Remote Sensing 12, 765. https://doi.org/10.3390/rs12050765.

Coulibaly, I., Spiric, N., Lepage, R., St-Jacques, M., 2017. Semiautomatic road extraction from Vhr images based on multiscale and spectral angle in case of earthquake. IEEE J. Sel. Top. Appl. Earth Obs. Remote Sens. 11 (1), 238–248. https://doi.org/10.1109/JSTARS.2017.2760282.

Courtrai, L., Lefèvre, S., 2016. Morphological path filtering at the region scale for efficient and robust road network extraction from satellite imagery. Pattern Recogn. Lett. 83, 195–204. https://doi.org/10.1016/j.patrec.2016.05.014.

Cramer, M., 2010. The Dgpf-test on digital airborne camera evaluation - over- view and test design. Photogrammetrie Fernerkundung Geoinformation 2010 (2), 73–82.

Cui F., Feng R., Wang L., and Wei L. 2021. "Joint Superpixel Segmentation and Graph Convolutional Network Road Extration for High-Resolution Remote Sensing Imagery," Paper presented at the 2021 IEEE International Geoscience and Remote Sensing Symposium IGARSS, Brussels, Belgium, 11-16 July 2021. 10.1109/IGARSS47720.2021.9554635.

Dai, J., Ma, R., Gong, L., Shen, Z., Wu, J., 2021. A model-driven-to-sample-driven method for rural road extraction. Remote Sens. 13, 1417. https://doi.org/10.3390/RS13081417.

Dai, J., Zhu, T., Wang, Y., Ma, R., Fang, X., 2020a. Road extraction from high-resolution satellite images based on multiple descriptors. IEEE J. Sel. Top. Appl. Earth Obs. Remote Sens. 13, 227–240. https://doi.org/10.1109/JSTARS.2019.2955277.

Dai, J., Li, C., Zuo, Y., Ai, H., 2020b. An Osm data-driven method for road-positive sample creation. Remote Sens. 12, 3612. https://doi.org/10.3390/rs12213612.

Dai, J., Zhu, T., Zhang, Y., Ma, R., Li, W., 2019. Lane-level road extraction from high-resolution optical satellite images. Remote Sens. 11 (22), 2672. https://doi.org/10.3390/rs11222672.

Das, S., Mirnalinee, T.T., Varghese, K., 2011. Use of salient features for the design of a multistage framework to extract roads from high-resolution multispectral satellite images. IEEE Trans. Geosci. Remote Sens. 49, 3906–3931. https://doi.org/10.1109/TGRS.2011.2136381.

Demir I., Koperski K., Lindenbaum D., Pang G., Huang J., Basu S., Hughes F., Tuia D., Raska R., 2018. Deepglobe 2018: A Challenge to Parse the Earth through Satellite Images. In: Paper presented at the 2018 IEEE/CVF Conference on Computer Vision and Pattern Recognition Workshops (CVPRW).

Deng X.-p., He C., Sun H., 2010. An Improved Gvf Snake Model and Its Application to Linear Feature Extraction from Sar Images. Paper presented at the IEEE 10th international conference on signal processing proceedings, Beijing, China, 24-28 Oct. 2010. 10.1109/ICOSP.2010.5655726.

Ding, L., Bruzzone, L., 2020. DiResNet: direction-aware residual network for road extraction in VHR remote sensing images. IEEE Trans. Geosci. Remote Sensing 59 (12), 10243–10254.

El-Halawany S., Moussa A., Lichti D. D., and El-Sheimy N., 2011. Detection of Road Curb from Mobile Terrestrial Laser Scanner Point Cloud. In: Paper presented at the 2011 ISPRS Workshop on Laser Scanning, Calgary, AB, Canada, 29–31 August 2011. 10.5194/ISPRSARCHIVES-XXXVIII-5-W12-109-2011.

Etten A.V., Lindenbaum D., Bacastow T.M., 2018, "Spacenet: A Remote Sensing Dataset and Challenge Series. ArXiv, vol. abs/1807.01232.

Ferraz, A., Mallet, C., Chehata, N., 2016. Large-scale road detection in forested mountainous areas using airborne topographic lidar data. ISPRS J. Photogramm. Remote Sens. 112, 23–36. https://doi.org/10.1016/j.isprsjprs.2015.12.002.

Fu, J., Liu, J., Tian, H., Li, Y., Bao, Y., Fang, Z., Lu, H., 2019. Dual Attention Network for Scene Segmentation. In: Paper presented at the 2019 IEEE/CVF Conference on Computer Vision and Pattern Recognition (CVPR), Long Beach, CA, USA, 15-20 June 2019. 10.1109/cvpr.2019.00326.

Gao, L., Wang, J., Wang, Q., Shi, W., Zheng, J., Gan, H., Lv, Z., Qiao, H., 2021a. Road Extraction using a dual attention dilated-linknet based on satellite images and floating vehicle trajectory data. IEEE J. Select. Top. Appl. Earth Observ. Remote Sens. 14, 10428–10438. https://doi.org/10.1109/jstars.2021.3116281.

Gao, L., Shi, W., Zhu, J., Shao, P., Sun, S., Li, Y., Wang, F., Gao, F., 2021b. Novel framework for 3d road extraction based on airborne lidar and high-resolution remote sensing imagery. Remote Sens. 13 (23), 4766. https://doi.org/10.3390/rs13234766.

Gao, L., Song, W., Dai, J., Chen, Y., 2019. Road extraction from high-resolution remote sensing imagery using refined deep residual convolutional neural network. Remote Sensing 11 (5), 552. https://doi.org/10.3390/rs11050552.

Geng, K., Sun, X., Yan, Z., Diao, W., Gao, X., 2020. Topological space knowledge distillation for compact road extraction in optical remote sensing images. Remote Sens. 12, 3175. https://doi.org/10.3390/rs12193175.

Grinias, I., Panagiotakis, C., Tziritas, G., 2016. Mrf-based segmentation and unsupervised classification for building and road detection in peri-urban areas of high-resolution satellite images. ISPRS J. Photogramm. Remote Sens. 122, 145–166. https://doi.org/10.1016/J.ISPRSJPRS.2016.10.010.

Gu, J., Wang, Y., Chen, L., Zhao, Z., Xuanyuan, Z., Huang, K., 2018a. A reliable road segmentation and edge extraction for sparse 3d lidar data. In: Paper presented at the 2018 IEEE Intelligent Vehicles Symposium (IV), Changshu, China, 26–30 June 2018. 130.10.1109/IVS.2018.8500486.

Gu, S., Lu, T., Zhang, Y., Alvarez, J.M., Yang, J., Kong, H., 2018b. 3-D Lidar + monocular camera: an inverse-depth-induced fusion framework for urban road detection. IEEE Trans. Intell. Veh. 3, 351–360. https://doi.org/10.1109/TIV.2018.2843170.

Gu, S., Zhang, Y., Yang, J., Kong, H., Paris, France,6-8 Sept. 2017 2017, "Lidar-Based Urban Road Detection by Histograms of Normalized Inverse Depths and Line Scanning. In: 2017 European Conference on Mobile Robots (ECMR), pp. 1-6. 10.1109/ECMR.2017.8098682.

Guan, H., Li, J., Yu, Y., Cheng, W., Chapman, M., Yang, B., 2014. Using mobile laser scanning data for automated extraction of road markings. ISPRS J. Photogramm. Remote Sens. 87, 93–107. https://doi.org/10.1016/J.ISPRSJPRS.2013.11.005.

Guan, Haiyan, Li, J., Yongtao Yu, Chapman, M., Cheng Wang, 2015. Automated road information extraction from mobile laser scanning data. IEEE Trans. Intell. Transp. Syst. 16 (1), 194–205.

Guo, J., Tsai, M.J., Han, J.Y., 2015. Automatic reconstruction of road surface features by using terrestrial mobile lidar. Autom. Constr. 58, 165–175. https://doi.org/10.1016/J.AUTCON.2015.07.017.

Guo, Q., Wang, Z., 2020. A self-supervised learning framework for road centerline extraction from high-resolution remote sensing images. IEEE J. Sel. Top. Appl. Earth Obs. Remote Sens. 13, 4451–4461. https://doi.org/10.1109/JSTARS.2020.3014242.

Han X., Wang H., Lu J., Zhao C., 2017. Road detection based on the fusion of lidar and image data. Int. J. Adv. Robot. Syst. 14(6). 10.1177/1729881417738102.

He, C., Yang, F., Yin, S., Deng, X.-P., Liao, M., 2013. Stereoscopic road network extraction by decision-level fusion of optical and Sar imagery. IEEE J. Sel. Top. Appl. Earth Obs. Remote Sens. 6, 2221–2228. https://doi.org/10.1109/JSTARS.2013.2249656.

He, C., Liao, Z., Yang, F., Deng, X.-P., Liao, M., 2012. Road extraction from Sar imagery based on multiscale geometric analysis of detector responses. IEEE J. Sel. Top. Appl. Earth Obs. Remote Sens. 5, 1373–1382. https://doi.org/10.1109/JSTARS.2012.2219614.

He, C., Shi, B., Zhang, Y., Xu, X., Liao, M., 2014. Road extraction for Sar imagery based on the combination of beamlet and a selected kernel. In: Paper presented at the 2014 IEEE Geoscience and Remote Sensing Symposium, Quebec City, QC, Canada, 13-18 July 2014. 10.1109/IGARSS.2014.6946919.

He, H., Yang, D., Wang, S., Wang, S., Li, Y., 2019. Road extraction by using atrous spatial pyramid pooling integrated encoder-decoder network and structural similarity loss. Remote Sens. 11, 1015. https://doi.org/10.3390/RS11091015.

He, W., Song, H., Yao, Y., Jia, X., 2021. A multiscale method for road network extraction from high-resolution Sar images based on directional decomposition and regional quality evaluation. Remote Sens. 13 (8), 1476. https://doi.org/10.3390/RS13081476.

Henry, C., Azimi, S., Merkle, N., 2018. Road segmentation in Sar satellite images with deep fully convolutional neural networks. IEEE Geosci. Remote Sens. Lett. 15, 1867–1871. https://doi.org/10.1109/LGRS.2018.2864342.

Hervieu, A., Soheilian, B., 2013a. Semi-automatic road/pavement modeling using mobile laser scanning. In: ISPRS Annals of the Photogrammetry, Remote Sensing and Spatial Information Sciences II-3/W3, 31–36. 10.5194/ISPRSANNALS-II-3-W3-31-2013.

Hervieu, A., Soheilian, B., 2013b. Road Side Detection and Reconstruction Using Lidar Sensor. In: Paper presented at the IEEE Intelligent Vehicles Symposium (IV), Gold Coast, 23 June 2013. 10.1109/IVS.2013.6629637.

Hinton G.E., Vinyals, O., Dean, J., 2015. Distilling the Knowledge in a Neural Network. ArXiv, vol. abs/1503.02531.

Hormese, J., Saravanan, C., 2016. Automated road extraction from high resolution satellite images. Procedia Technol. 24, 1460–1467. https://doi.org/10.1016/J.PROTCY.2016.05.180.

Hu, A., Chen, S., Wu, L., Xie, Z., Qiu, Q., Xu, Y., 2021. Wsgan: an improved generative adversarial network for remote sensing image road network extraction by weakly supervised processing. Remote Sens. 13, 2506. https://doi.org/10.3390/rs13132506.

Hu, S., Chen, H., Wang, B., Gong, J., Ma, Y., 2020. Lidar-based road extraction for ugv in high definition map. In: Paper presented at the 2020 3rd International Conference on Unmanned Systems (ICUS), Harbin, China, 27-28 November 2020. 10.1109/ICUS50048.2020.9274830.

Hu, X., Li, Y., Shan, J., Zhang, J., Zhang, Y., 2014. Road centerline extraction in complex urban scenes from lidar data based on multiple features. IEEE Trans. Geosci. Remote Sens. 52 (11), 7448–7456. https://doi.org/10.1109/TGRS.2014.2312793.

Huang, J., Choudhury, P.K., Yin, S., Zhu, L., 2021. Real-time road curb and lane detection for autonomous driving using lidar point clouds. IEEE Access 9, 144940–144951. https://doi.org/10.1109/access.2021.3120741.

Huang, R., Chen, J., Liu, J., Liu, L., Yu, B., Wu, Y., 2017. A practical point cloud based road curb detection method for autonomous vehicle. Information Fusion 8 (3), 93. https://doi.org/10.3390/info8030093.

Huang, S., Xiong, G., Zhu, B., Gong, J., Chen, H., 2020. Lidar-camera fusion based high-resolution network for efficient road segmentation. In: Paper presented at the 2020 3rd International Conference on Unmanned Systems (ICUS), Harbin, China, 27-28 Nov. 2020. 10.1109/ICUS50048.2020.9274954.

Hui, Z., Hu, Y., Jin, S., Yao, Z.Y., 2016. Road centerline extraction from airborne lidar point cloud based on hierarchical fusion and optimization. ISPRS J. Photogramm. Remote Sens. 118, 22–36. https://doi.org/10.1016/J.ISPRSJPRS.2016.04.003.

Husain, A., Vaishya, R.C., 2018. Road surface and its center line and boundary lines detection using terrestrial lidar data. Egypt. J. Remote Sens. Space Sci. 21, 363–374. https://doi.org/10.1016/j.ejrs.2017.12.005.

Jayaseeli, J., Malathi, D., Gopika, S., 2018. Road extraction using deep learning. Int. J. Eng. Technol. 7, 1079. 10.14419/ijet.v7i4.10.27923.

Jiang, M., Miao, Z., Gamba, P., Yong, B., 2017. Application of multitemporal insar covariance and information fusion to robust road extraction. IEEE Trans. Geosci. Remote Sens. 55, 3611–3622. https://doi.org/10.1109/TGRS.2017.2677260.

Jing, R., Gong, Z., Zhu, W., Guan, H., Zhao, W., 2018. Island road centerline extraction based on a multiscale united feature. IEEE J. Sel. Top. Appl. Earth Obs. Remote Sens. 11, 3940–3953. https://doi.org/10.1109/JSTARS.2018.2872520.

Jung, Y., Seo, S.-W., Kim, S.-W., 2020. Curb detection and tracking in low-resolution 3d point clouds based on optimization framework. IEEE Trans. Intell. Transp. Syst. 21 (9), 3893–3908. https://doi.org/10.1109/tits.2019.2938498.

Kang, Y., Roh, C., Suh, S.B., ong, B., 2012. A lidar-based decision-making method for road boundary detection using multiple kalman filters. IEEE Trans. Ind. Electron. 59 (11),4360-4368. 10.1109/TIE.2012.2185013.

Kearney, S.P., Coops, N.C., Sethi, S., Stenhouse, G.B., 2020. Maintaining accurate, current, rural road network data: an extraction and updating routine using rapideye, participatory Gis and deep learning. Int. J. Appl. Earth Obs. Geoinf. 87, 102031 https://doi.org/10.1016/j.jag.2019.102031.

Kestur, R., Farooq, S., Abdal, R., Mehraj, E., Narasipura, O.S., Mudigere, M., 2018. Ufcn: a fully convolutional neural network for road extraction in rgb imagery acquired by remote sensing from an unmanned aerial vehicle. J. Appl. Remote Sens. 12 (1), 016020 https://doi.org/10.1117/1.JRS.12.016020.

Khesali, E., Zoej, M.J.V., Mokhtarzade, M., Dehghani, M., 2016. Semi automatic road extraction by fusion of high resolution optical and radar images. J. Indian Soc. Remote Sens. 44 (1), 21–29. https://doi.org/10.1007/s12524-015-0480-2.

Koch, M.W., Moya, M.M., Chow, J.G., Goold, J., Malinas, R., 2015. Road segmentation using multipass single-pol synthetic aperture radar imagery. In: Paper presented at the Proceedings of the IEEE Conference on Computer Vision and Pattern Recognition Workshops, Boston, MA, USA, 7-12 June 2015. 10.1109/CVPRW.2015.7301309.

Krylov, V.A., Nelson, J.D.B., 2014. Stochastic extraction of elongated curvilinear structures with applications. IEEE Trans. Image Process. 23, 5360–5373. https://doi.org/10.1109/TIP.2014.2363612.

Kukolj, D., Marinović, I., Nemet, S., 2021. Road edge detection based on combined deep learning and spatial statistics of lidar data. J. Spat. Sci. 1-15. 10.1080/14498596.2021.1960912.

Kumar, P., McElhinney, C.P., Lewis, P., McCarthy, T., 2013. An automated algorithm for extracting road edges from terrestrial mobile lidar data. ISPRS J. Photogramm. Remote Sens. 85, 44–55. https://doi.org/10.1016/j.isprsjprs.2013.08.003.

Kumar, P., Mccarthy, T., Elhinney, C., 2010. Automated road extraction from terrestrial based mobile laser scanning system using the Gvf Snake Model. Paper presented at the European LiDAR Mapping Forum, The Netherlands, November, p. 2010.

Kumar, P., Lewis, P., McElhinney, C.P., Boguslawski, P., McCarthy, T., 2017. Snake energy analysis and result validation for a mobile laser scanning data-based automated road edge extraction algorithm. IEEE J. Sel. Top. Appl. Earth Obs. Remote Sens. 10, 763–773. https://doi.org/10.1109/JSTARS.2016.2564984.

Lachachi, M.Y., Ouslim, M., Niar, S., Taleb-Ahmed, A., 2018. Lidar and Stereo-Camera Fusion for Reliable Road Extraction. In: Paper presented at the 2018 30th International Conference on Microelectronics (ICM), Tunisia, December 16 - 19, 2018. 177.10.1109/ICM.2018.8704114.

Leela, A.T., Panda, M., 2020. Road Boundary Detection Using 3d-to-2d Transformation of Lidar Data and Conditional Generative Adversarial Networks. In: Paper presented at the 2020 11th International Conference on Computing, Communication and Networking Technologies (ICCCNT), Kharagpur, India, 1-3 July 2020. 10.1109/ICCCNT49239.2020.9225268.

Leninisha, S., Vani, K., 2015. Water flow based geometric active deformable model for road network. ISPRS J. Photogramm. Remote Sens. 102, 140–147. https://doi.org/10.1016/J.ISPRSJPRS.2015.01.013.

Li, C., Lian, M., Mei, Z., Zhu, X., 2016a. Study on road detection method from full-waveform lidar data in forested area. In: Paper presented at the Fourth International Conference on Ubiquitous Positioning, Shanghai, China, 2-4 Nov. 2016. 10.1109/UPINLBS.2016.7809978.

Li, H., Chen, Y., Zhang, Q., Zhao, D., 2021a. Bifnet: bidirectional fusion network for road segmentation. IEEE Trans. Cybernet. PP. 10.1109/TCYB.2021.3105488.

Li, J., Liu, Y., Zhang, Y., Zhang, Y., 2021b. Cascaded attention denseunet (Cadunet) for road extraction from very-high-resolution images. ISPRS Int. J. Geo-Inf. 10, 329. https://doi.org/10.3390/ijgi10050329.

Li, L., Lim, S., 2014. A novel algorithm for road extraction from airborne lidar data. In: Paper presented at the 14th Environmental Science, Canberra, Australia, 07-09 April 2014.

Li, M., Stein, A., Bijker, W., Zhan, Q., 2016b. Region-based urban road extraction from vhr satellite images using binary partition tree. Int. J. Appl. Earth Obs. Geoinf. 44, 217–225. https://doi.org/10.1016/j.jag.2015.09.005.

Li, P., He, X., Qiao, M., Cheng, X., Li, Z., Luo, H., Song, D., Li, D., Hu, S., Li, R., Han, P., Qiu, F., Guo, H., Shang, J., Tian, Z., 2021c. Robust deep neural networks for road extraction from remote sensing images. IEEE Trans. Geosci. Remote Sens. 59, 6182–6197. https://doi.org/10.1109/TGRS.2020.3023112.

Li, P., He, X., Qiao, M., Miao, D., Cheng, X., Song, D., Chen, M., Li, J., Zhou, T., Guo, X., Yan, X., Tian, Z., 2021d. Exploring multiple crowdsourced data to learn deep convolutional neural networks for road extraction. Int. J. Appl. Earth Obs. Geoinf. 104, 102544 https://doi.org/10.1016/j.jag.2021.102544.

Li, R., Gao, B., Xu, Q., 2021e. Gated auxiliary edge detection task for road extraction with weight-balanced Loss. IEEE Geosci. Remote Sens. Lett. 18, 786–790. https://doi.org/10.1109/LGRS.2020.2985774.

Li, X., Zhang, S., Pan, X., Dale, P., Cropp, R., 2010. Straight road edge detection from high-resolution remote sensing images based on the ridgelet transform with the revised parallel-beam radon transform. Int. J. Remote Sens. 31, 5041–5059. https://doi.org/10.1080/01431160903283835.

Li, X., Wang, Y., Zhang, L., Liu, S., Mei, J., Li, Y., 2020. Topology-enhanced urban road extraction via a geographic feature-enhanced network. IEEE Trans. Geosci. Remote Sens. 58, 8819–8830. https://doi.org/10.1109/TGRS.2020.2991006.

Li, Y., Xu, L., Rao, J., Guo, L., Yan, Z., Jin, S., 2019a. A Y-net deep learning method for road segmentation using high-resolution visible remote sensing images. Remote Sens. Lett. 10, 381–390. https://doi.org/10.1080/2150704X.2018.1557791.

Li, Y., Hu, X., Guan, H., Liu, P., 2016c. An efficient method for automatic road extraction based on multiple features from lidar data. ISPRS - International Archives of the Photogrammetry, Remote Sensing and Spatial Information Sciences, vol. XLI-B3, pp. 289-293. 10.5194/isprsarchives-XLI-B3-289-2016.

Li, Y., Yong, B., Wu, H., An, R., Xu, H., 2015. Road detection from airborne lidar point clouds adaptive for variability of intensity data. Optik-Int. J. Light Electron Opt. 126 (23), 4292–4298. https://doi.org/10.1016/j.ijleo.2015.08.137.

Li, Y., Guo, L., Rao, J., Xu, L., Jin, S., 2019b. Road segmentation based on hybrid convolutional network for high-resolution visible remote sensing image. IEEE Geosci. Remote Sens. Lett. 16, 613–617. https://doi.org/10.1109/LGRS.2018.2878771.

Lian, R., Wang, W., Mustafa, N., Huang, L., 2020. Road extraction methods in high-resolution remote sensing images: a comprehensive review. IEEE J. Sel. Top. Appl. Earth Obs. Remote Sens. 13, 5489–5507. https://doi.org/10.1109/JSTARS.2020.3023549.

Lian, R., Huang, L., 2020. Deepwindow: sliding window based on deep learning for road extraction from remote sensing images. IEEE J. Sel. Top. Appl. Earth Obs. Remote Sens. 13, 1905–1916. https://doi.org/10.1109/JSTARS.2020.2983788.

Liang, J., Homayounfar, N., Ma, W., Wang, S., Urtasun, R., 2019. Convolutional Recurrent Network for Road Boundary Extraction. In: 2019 IEEE/CVF Conference on Computer Vision and Pattern Recognition (CVPR), pp. 9504-9513. 10.1109/CVPR.2019.00974.

Lin, Y., Wan, L., Zhang, H., Wei, S., Ma, P., Li, Y., Zhao, Z., 2021. Leveraging optical and sar data with a Uu-net for large-scale road extraction. Int. J. Appl. Earth Obs. Geoinf. 103, 102498 https://doi.org/10.1016/j.jag.2021.102498.

Liu, J., Sui, H., Tao, M., Sun, K., Mei, X., 2013. Road extraction from sar imagery based on an improved particle filtering and snake model. Int. J. Remote Sens. 34 (22), 8199–8214. https://doi.org/10.1080/01431161.2013.835082.

Liu, L., Lim, S., 2017. Color component-based road feature extraction from airborne lidar and imaging data sets. J. Surv. Eng. 143, 04016021. https://doi.org/10.1061/(ASCE)SU.1943-5428.0000198.

Liu, L., Lim, S., 2016. A framework of road extraction from airborne lidar data and aerial imagery. J. Spat. Sci. 61, 263–281. https://doi.org/10.1080/14498596.2016.1147392.

Liu, R., Miao, Q., Song, J., Quan, Y., Li, Y., Xu, P., Dai, J., 2019. Multiscale road centerlines extraction from high-resolution aerial imagery. Neurocomputing 329, 384–396. https://doi.org/10.1016/j.neucom.2018.10.036.

Liu, R., Song, J., Miao, Q., Xu, P., Xue, Q., 2016. Road centerlines extraction from high resolution images based on an improved directional segmentation and road probability. Neurocomputing 212, 88–95. https://doi.org/10.1016/j.neucom.2016.03.095.

Liu, Y., Yao, J., Lu, X., Xia, M., Wang, X., Liu, Y., 2018. Roadnet: learning to comprehensively analyze road networks in complex urban scenes from high-resolution remotely sensed images. IEEE Trans. Geosci. Remote Sens. 57 (4), 2043–2056. https://doi.org/10.1109/TGRS.2018.2870871.

Long, J., Shelhamer, E., Darrell, T., 2017. Fully convolutional networks for semantic segmentation. IEEE Trans. Pattern Anal. Mach. Intell. 39 (4), 640–651.

Lu, P., Du, K., Yu, W., Wang, R., Deng, Y., Balz, T., 2014. A new region growing-based method for road network extraction and its application on different resolution Sar images. IEEE J. Sel. Top. Appl. Earth Obs. Remote Sens. 7 (12), 4772–4783. https://doi.org/10.1109/JSTARS.2014.2340394.

Lu, X., Zhong, Y., Zheng, Z., Zhang, L.-P., 2021a. Gamsnet: globally aware road detection network with multi-scale residual learning. ISPRS J. Photogramm. Remote Sens. 175, 340–352. https://doi.org/10.1016/J.ISPRSJPRS.2021.03.008.

Lu, X., Zhong, Y., Zheng, Z., Liu, Y., Zhao, J., Ma, A., Yang, J., 2019. Multi-scale and multi-task deep learning framework for automatic road extraction. IEEE Trans. Geosci. Remote Sens. 57 (11), 9362–9377. https://doi.org/10.1109/TGRS.2019.2926397.

Lu, X., Zhong, Y., Zheng, Z., Wang, J., 2021b. Cross-domain road detection based on global-local adversarial learning framework from very high resolution satellite imagery. ISPRS J. Photogramm. Remote Sens. https://doi.org/10.1016/j.isprsjprs.2021.08.018.

Lv, Z., Jia, Y., Zhang, Q., Chen, Y., 2017. An adaptive multifeature sparsity-based model for semiautomatic road extraction from high-resolution satellite images in urban areas. IEEE Geosci. Remote Sens. Lett. 14 (8), 1238–1242. https://doi.org/10.1109/LGRS.2017.2704120.

Lyu, Y., Bai, L., Huang, X., 2018. Real-Time Road Segmentation Using Lidar Data Processing on an Fpga. In: Paper presented at the 2018 IEEE International Symposium on Circuits and Systems (ISCAS), Florence, Italy, 27–30 May. 10.1109/ISCAS.2018.8351244.

Ma, L., Li, Y., Li, J., Junior, J.M., Goncalves, W.N., Chapman, M.A., 2021. Boundarynet: extraction and completion of road boundaries with deep learning using mobile laser scanning point clouds and satellite imagery. IEEE Trans. Intell. Transport. Syst. 1–17. 10.1109/tits.2021.3055366.

Ma, L., Li, J., Li, Y., Zhong, Z., Chapman, M., 2019. Generation of horizontally curved driving lines in Hd maps using mobile laser scanning point clouds. IEEE J. Sel. Top. Appl. Earth Obs. Remote Sens. 12, 1572–1586. https://doi.org/10.1109/JSTARS.2019.2904514.

Maboudi, M., Amini, J., Malihi, S., Hahn, M., 2018. Integrating fuzzy object based image analysis and ant colony optimization for road extraction from remotely sensed images. ISPRS J. Photogramm. Remote Sens. 138, 151–163. https://doi.org/10.1016/J.ISPRSJPRS.2017.11.014.

Maboudi, M., Amini, J., Hahn, M., Saati, M., 2016. Road network extraction from Vhr satellite images using context aware object feature integration and tensor voting. Remote Sensing 8 (8), 637. https://doi.org/10.3390/rs8080637.

Manandhar, P., Marpu, P.R., Aung, Z., Melgani, F., 2019. Towards automatic extraction and updating of Vgi-based road networks using deep learning. Remote Sens. 11, 1012. https://doi.org/10.3390/RS11091012.

Matkan, A.A., Hajeb, M., Sadeghian, S., 2014. Road extraction from lidar data using support vector machine classification. Photogramm. Eng. Remote Sens. 80 (5), 409–422. https://doi.org/10.14358/pers.80.5.409.

Mi, X., Yang, B., Dong, Z., Chen, C., Gu, J., 2021, Automated 3d road boundary extraction and vectorization using Mls point clouds. IEEE Trans. Intell. Transport. Syst. pp. 1-11. 10.1109/tits.2021.3052882.

Miao, Z., Shi, W., Zhang, H., Wang, X., 2013. Road centerline extraction from high-resolution imagery based on shape features and multivariate adaptive regression splines. IEEE Geosci. Remote Sens. Lett. 10, 583–587. https://doi.org/10.1109/LGRS.2012.2214761.

Miao, Z., Wang, B., Shi, W., Wu, H., 2014a. A method for accurate road centerline extraction from a classified image. IEEE J. Sel. Top. Appl. Earth Obs. Remote Sens. 7, 4762–4771. https://doi.org/10.1109/JSTARS.2014.2309613.

Miao, Z., Shi, W., Gamba, P., Li, Z., 2015. An object-based method for road network extraction in Vhr satellite images. IEEE J. Sel. Top. Appl. Earth Obs. Remote Sens. 8 (10), 4853–4862. https://doi.org/10.1109/JSTARS.2015.2443552.

Miao, Z., Wang, B., Shi, W., Zhang, H., 2014b. A semi-automatic method for road centerline extraction from Vhr images. IEEE Geosci. Remote Sens. Lett. 11, 1856–1860. https://doi.org/10.1109/LGRS.2014.2312000.

Miraliakbari, A., Hahn, M., Sok, S., 2015. Automatic extraction of road surface and curbstone edges from mobile laser scanning data. Int. Arch. Photogram. Remote Sens. Spat. Inform. Sci. vol. XL-4/W5, 119–124. https://doi.org/10.5194/isprsarchives-XL-4-W5-119-2015.

Mnih, V., 2015. Machine Learning for Aerial Image Labeling [Online] Available: http://www.cs.toronto.edu/~vmnih/data/.

Movaghati, S., Moghaddamjoo, A., Tavakoli, A., 2010. Road extraction from satellite images using particle filtering and extended kalman filtering. IEEE Trans. Geosci. Remote Sens. 48 (7), 2807–2817. https://doi.org/10.1109/TGRS.2010.2041783.

Mu, H., Zhang, Y., Li, H., Guo, Y., Zhuang, Y., 2016. Road Extraction Base on Zernike Algorithm on Sar Image. Paper presented at the 2016 IEEE International Geoscience and Remote Sensing Symposium (IGARSS), Beijing, China, 10-15 July 2016. 10.1109/IGARSS.2016.7729323.

Narwade, R.D., Musande, V., 2014. Road extraction from airborne lidar data using Sbf and Cd-Tin. In: Paper presented at the 2014 International Conference on Advances in Computing, Communications and Informatics (ICACCI), New Delhi, 24-27 Sept., 2014. 10.1109/ICACCI.2014.6968515.

Oktay, O., Schlemper, J., Folgoc, L.L., Lee, M., Heinrich, M., Misawa, K., Mori, K., McDonagh, S., Hammerla, N.Y., Kainz, B., 2018, Attention U-net: learning where to look for the pancreas. arXiv preprint arXiv:1804.03999.

Ouyang, S., Li, Y., 2021. Combining deep semantic segmentation network and graph convolutional neural network for semantic segmentation of remote sensing imagery. Remote Sensing 13, 119. https://doi.org/10.3390/rs13010119.

Pan, D., Zhang, M., Zhang, B., 2021. A generic Fcn-based approach for the road-network extraction from Vhr remote sensing images using openstreetmap as benchmarks. IEEE J. Sel. Top. Appl. Earth Obs. Remote Sens. 14, 2662–2673. https://doi.org/10.1109/JSTARS.2021.3058347.

Pan, H., Jia, Y., Lv, Z., 2019. An adaptive multifeature method for semiautomatic road extraction from high-resolution stereo mapping satellite images. IEEE Geosci. Remote Sens. Lett. 16 (2), 201–205. https://doi.org/10.1109/LGRS.2018.2870488.

Panboonyuen, T., Jitkajornwanich, K., Lawawirojwong, S., Srestasathiern, P., Vateekul, P., 2017. Road segmentation of remotely-sensed images using deep convolutional neural networks with landscape metrics and conditional random fields. Remote Sensing 9, 680. https://doi.org/10.3390/rs9070680.

Perciano, T., Tupin, F., Hirata Jr, R., Cesar Jr, R.M., 2016. A two-level markov random field for road network extraction and its application with optical, Sar, and multitemporal data. Int. J. Remote Sens. 37 (16), 3584–3610. https://doi.org/10.1080/01431161.2016.1201227.

Poulain, V., Inglada, J., Spigai, M., Tourneret, J.-Y., Marthon, P., 2010. High resolution optical and sar image fusion for road database updating. In: Paper presented at the 2010 IEEE International Geoscience and Remote Sensing Symposium, Honolulu, HI, USA, 25-30 July 2010. 10.1109/IGARSS.2010.5653251.

Poullis, C., 2014. Tensor-cuts: a simultaneous multi-type feature extractor and classifier and its application to road extraction from satellite images. ISPRS J. Photogramm. Remote Sens. 95 (95), 93–108. https://doi.org/10.1016/J.ISPRSJPRS.2014.06.006.

Poullis, C., You, S., 2010. Delineation and geometric modeling of road networks. ISPRS J. Photogramm. Remote Sens. 65, 165–181. https://doi.org/10.1016/J.ISPRSJPRS.2009.10.004.

Prendes, C., Buján, S., Ordoñez, C., Canga, E., 2019. Large scale semi-automatic detection of forest roads from low density lidar data on steep Terrain in Northern Spain. iForest - Biogeosciences and Forestry 12 (4), 366–374. https://doi.org/10.3832/ifor2989-012.

Previtali, M., Barazzetti, L., Scaioni, M., 2020. Automated road information extraction from high resolution aerial Lidar data for smart road applications. Int. Arch. Photogram. Remote Sens. Spatial Inform. Sci. XLIII-B3-2020, 533–539. https://doi.org/10.5194/isprs-archives-XLIII-B3-2020-533-2020.

Pu, S., Rutzinger, M., Vosselman, G., Elberink, S.O., 2011. Recognizing basic structures from mobile laser scanning data for road inventory studies. ISPRS J. Photogramm. Remote Sens. 66 (6S), S28–S39. https://doi.org/10.1016/J.ISPRSJPRS.2011.08.006.

Qiu, K., Kai, S., Kou, D., Zhen, S., 2016. A fast and robust algorithm for road edges extraction from lidar data. ISPRS – Int. Arch. Photogram. Remote Sens. Spat. Inf. Sci. vol. XLI-B5, 693–698. https://doi.org/10.5194/isprsarchives-XLI-B5-693-2016.

Rato, D., Santos, V., 2021. Lidar based detection of road boundaries using the density of accumulated point clouds and their gradients. Robot. Autonomous Syst. 138, 103714 https://doi.org/10.1016/j.robot.2020.103714.

Ren, Y., Yu, Y., Guan, H., 2020. Da-capsunet: a dual-attention capsule U-net for road extraction from remote sensing imagery. Remote Sens. 12 (18), 2866. https://doi.org/10.3390/rs12182866.

Rochan, M.R.A., K.A. Sujatha, J., 2018. Multi sensor based approach for road region extraction for autonomous vehicles. In: Paper presented at the 2018 10th International Conference on Knowledge and Smart Technology (KST), Chiang Mai, Thailand, 31 Jan.-3 Feb. 2018. 10.1109/KST.2018.8426155.

RodrguezCuenca, 2015. An approach to detect and delineate street curbs from Mls 3d point cloud data. Automat. Construct. 51, 103-112. 10.1016/J.AUTCON.2014.12.009.

Ronneberger, O., Fischer, P., Brox, T., 2015. U-Net: convolutional networks for biomedical image segmentation. In: Paper presented at the medical image computing and computer-assisted intervention – MICCAI 2015, Munich, Germany, 5-9 October 2015.

Saati, M., Amini, J., Maboudi, M., 2015. A method for automatic road extraction of high resolution Sar imagery. J. Ind. Soc. Remote Sens. 43 (4), 697–707. https://doi.org/10.1007/s12524-015-0454-4.

Sánchez, J.M., Rivera, F.F., Domínguez, J.C., Vilariño, D.L., Pena, T.F., 2020. Automatic extraction of road points from airborne lidar based on bidirectional skewness balancing. Remote Sens. 12 (12), 2025. https://doi.org/10.3390/rs12122025.

Senthilnath, J., Varia, N., Dokania, A., Anand, G., Benediktsson, J.A., 2020. Deep tec: deep transfer learning with ensemble classifier for road extraction from Uav imagery. Remote Sensing 12 (2), 245. https://doi.org/10.3390/rs12020245.

Sghaier, M.O., Lepage, R., 2016. Road extraction from very high resolution remote sensing optical images based on texture analysis and beamlet transform. IEEE J. Sel.

Top. Appl. Earth Obs. Remote Sens. 9 (5), 1946–1958. https://doi.org/10.1109/JSTARS.2015.2449296.
Sha, Z., Chen, Y., Lin, Y., Wang, C., Marcato, J., Li, J., 2022. A supervoxel approach to road boundary enhancement from 3-D lidar point clouds. IEEE Geosci. Remote Sens. Lett. 19, 1–5. https://doi.org/10.1109/lgrs.2020.3037484.
Shamsolmoali, P., Zareapoor, M., Zhou, H., Wang, R., Yang, J., 2021. Road segmentation for remote sensing images using adversarial spatial pyramid networks. IEEE Trans. Geosci. Remote Sens. 59, 4673–4688. https://doi.org/10.1109/TGRS.2020.3016086.
Shao, Y., Guo, B., Hu, X., Di, L., 2011. Application of a fast linear feature detector to road extraction from remotely sensed imagery. IEEE J. Select. Top. Appl. Earth Observat. Remote Sens. 4, 626–631. https://doi.org/10.1109/JSTARS.2010.2094181.
Shao, Z., Zhou, Z., Huang, X., Zhang, Y., 2021. Mrenet: simultaneous extraction of road surface and road centerline in complex urban scenes from very high-resolution images. Remote Sens. 13, 239. https://doi.org/10.3390/rs13020239.
Shi, W., Miao, Z., Debayle, J., 2014a. An integrated method for urban main-road centerline extraction from optical remotely sensed imagery. IEEE Trans. Geosci. Remote Sens. 52, 3359–3372. https://doi.org/10.1109/TGRS.2013.2272593.
Shi, W., Miao, Z., Wang, Q., Zhang, H., 2014b. Spectral spatial classification and shape features for urban road centerline extraction. IEEE Geosci. Remote Sens. Lett. 11, 788–792. https://doi.org/10.1109/LGRS.2013.2279034.
Smadja, L., Ninot, J., Gavrilovic, T., 2010. Road extraction and environment interpretation from lidar sensors. ISPRS Achieves 38, 281–286.
Sun, P., Zhao, X., Xu, Z., Wang, R., Min, H., 2019a. A 3d lidar data-based dedicated road boundary detection algorithm for autonomous vehicles. IEEE Access 7, 29623–29638. https://doi.org/10.1109/ACCESS.2019.2902170.
Sun, T., Di, Z., Che, P., Liu, C., Wang, Y., 2019b. Leveraging crowdsourced gps data for road extraction from aerial imagery. 2019 IEEE/CVF Conference on Computer Vision and Pattern Recognition (CVPR), pp. 7501-7510. 10.1109/CVPR.2019.00769.
Sun, Z., Zhou, W., Ding, C., Xia, M., 2022. Multi-resolution transformer network for building and road segmentation of remote sensing image. ISPRS Int. J. Geo-Inf. 11 (3), 165. https://doi.org/10.3390/ijgi11030165.
Tan, X., Xiao, Z., Wan, Q., Shao, W., 2021. Scale sensitive neural network for road segmentation in high-resolution remote sensing images. IEEE Geosci. Remote Sens. Lett. 18, 533–537. https://doi.org/10.1109/LGRS.2020.2976551.
Tan, Y., Gao, S., Li, X.-y., Cheng, M.-M., Ren, B., 2020. Vecroad: Point-Based Iterative Graph Exploration for Road Graphs Extraction. In; Paper presented at the 2020 IEEE/CVF Conference on Computer Vision and Pattern Recognition (CVPR), Seattle, WA, USA, 13-19 June 2020. 10.1109/cvpr42600.2020.00893.
Tao, C., Qi, J., Li, Y., Wang, H., Li, H., 2019. Spatial information inference net: road extraction using road-specific contextual information. ISPRS J. Photogramm. Remote Sens. 158, 155–166. https://doi.org/10.1109/IGARSS.2019.8900507.
Tejenaki, S.A.K., Ebadi, H., Mohammadzadeh, A., 2019. A new hierarchical method for automatic road centerline extraction in urban areas using lidar data. Adv. Space Res. 64, 1792–1806. https://doi.org/10.1016/j.asr.2019.07.033.
Teo, T., Yu, H., 2015. Empirical radiometric normalization of road points from terrestrial mobile lidar system. Remote Sensing 7, 6336–6357. https://doi.org/10.3390/rs70506336.
Truong-Hong, L., Laefer, D.F., Lindenbergh, R.C., 2019. Automatic detection of road edges from aerial laser scanning data. Int. Arch. Photogram. Remote Sens. Spat. Inform. Sci. XLII-2/W13, 1135–1140. https://doi.org/10.5194/isprs-archives-XLII-2-W13-1135-2019.
Upadhayay, S., Yadav, M., Singh, D.P., 2018. Road network mapping using airborne lidar data. In: Paper presented at the ISPRS TC V Mid-term Symposium "Geospatial Technology – Pixel to People", Dehradun, India, 20–23 November 2018. 10.5194/isprs-archives-XLII-5-707-2018.
Valero, S., Chanussot, J., Benediktsson, J.A., Talbot, H., Waske, B., 2010. Advanced directional mathematical morphology for the detection of the road network in very high resolution remote sensing images. Pattern Recogn. Lett. 31 (10), 1120–1127. https://doi.org/10.1016/J.PATREC.2009.12.018.
Wang, G., Wu, J., He, R., Tian, B., 2021a. Speed and accuracy tradeoff for lidar data based road boundary detection. IEEE/CAA J. Autom. Sin. 8 (6), 1210–1220. https://doi.org/10.1109/jas.2020.1003414.
Wang, G., Zhang, Y., Li, J., 2011. 3d road information extraction from lidar data fused with aerial-images. In: Paper presented at the 2011 IEEE International Conference on Spatial Data Mining and Geographical Knowledge Services, Fuzhou, China, 29 June-1 July 2011. 183.10.1109/ICSDM.2011.5969064.
Wang, H., Cai, Z., Luo, H., Wang, C., Li, P., Yang, W., 2012. Automatic road extraction from mobile laser scanning data. In: Paper presented at the 2012 International Conference on Computer Vision in Remote Sensing, Xiamen, China, 16-18 Dec. 2012 10.1109/CVRS.2012.6421248.
Wang, H., Luo, H., Wen, C., Cheng, J., Li, P., Chen, Y., Wang, C., Li, J., 2015. Road boundaries detection based on local normal saliency from mobile laser scanning data. IEEE Geosci. Remote Sens. Lett. 12, 2085–2089. https://doi.org/10.1109/LGRS.2015.2449074.
Wang, Q., Gao, J., Yuan, Y., 2018. Embedding structured contour and location prior in siamesed fully convolutional networks for road detection. IEEE Trans. Intell. Transp. Syst. 19 (1), 230–241. https://doi.org/10.1109/TITS.2017.2749964.
Wang, S., Mu, X., Yang, D., He, H., Zhao, P., 2021b. Road extraction from remote sensing images using the inner convolution integrated encoder-decoder network and directional conditional random fields. Remote Sensing 13, 465. https://doi.org/10.3390/rs13030465.
Wang, X., Cavigelli, L., Eggimann, M., Magno, M., Benini, L., 2020. Hr-Sar-Net: A deep neural network for urban scene segmentation from high-resolution Sar data. In: Paper presented at the 2020 IEEE Sensors Applications Symposium (SAS), Kuala Lumpur, Malaysia, 9-11 March 2020. 10.1109/SAS48726.2020.9220068.
Wang, Y., Seo, J., Jeon, T., 2021c. Nl-linknet: toward lighter but more accurate road extraction with nonlocal operations. IEEE Geosci. Remote Sens. Lett. https://doi.org/10.1109/LGRS.2021.3050477.
Wegner, J.D., Montoya-Zegarra, J.A., Schindler, K., 2013. A higher-order Crf model for road network extraction. In: Paper presented at the 2013 IEEE Conference on Computer Vision and Pattern Recognition, Portland, OR, USA, 23-28 June 2013. 10.1109/CVPR.2013.222.
Wegner, J.D., Montoya-Zegarra, J.A., Schindler, K., 2015. Road networks as collections of minimum cost paths. ISPRS J. Photogramm. Remote Sens. 108, 128–137. https://doi.org/10.1016/J.ISPRSJPRS.2015.07.002.
Wei, X., Lv, X., Zhang, K., 2021. Road extraction in sar images using ordinal regression and road-topology loss. Remote Sensing 13, 2080. https://doi.org/10.3390/rs13112080.
Wei, Y., Ji, S., 2020. Scribble-based weakly supervised deep learning for road surface extraction from remote sensing images. IEEE Trans. Geosci. Remote Sens. 1-12. 10.1109/TGRS.2021.3061213.
Wei, Y., Zhang, K., Ji, S., 2020. Simultaneous road surface and centerline extraction from large-scale remote sensing images using Cnn-based segmentation and tracing. IEEE Trans. Geosci. Remote Sens. 58, 8919–8931. https://doi.org/10.1109/TGRS.2020.2991733.
Wulff, F., Schaufele, B., Sawade, O., 2018. Early fusion of camera and lidar for robust road detection based on U-Net Fcn. Paper presented at the 2018 IEEE Intelligent Vehicles Symposium (IV), Changshu, China, 26-30 June 2018. 10.1109/IVS.2018.8500549.
Xiao, F., Tong, L., Luo, S., 2019. A method for road network extraction from high-resolution sar imagery using direction grouping and curve fitting. Remote Sensing 11, 2733. https://doi.org/10.3390/rs11232733.
Xiao, F., Tong, L., 2019. A road extraction method using dual-temporal high-resolution Sar images. In: Paper presented at the IGARSS 2019 - 2019 IEEE International Geoscience and Remote Sensing Symposium, Yokohama, Japan, 28 July-2 Aug. 2019. 10.1109/IGARSS.2019.8900511.
Xiao, L., Dai, B., Liu, D., Hu T., Wu, T., 2015. Crf based road detection with multi-sensor fusion. In: Paper presented at the 2015 IEEE Intelligent Vehicles Symposium (IV), Seoul, Korea (South), 28 June-1 July 2015. 10.1109/IVS.2015.7225685.
Xiao, L., Wang, R., Dai, B., Fang, Y., Liu, D., Wu, T., 2017. Hybrid conditional random field based camera-lidar fusion for road detection. Inf. Sci. 432, 543–558. https://doi.org/10.1016/j.ins.2017.04.048.
Xin, J., Zhang, X., Zhang, Z., Fang, W., 2019. Road extraction of high-resolution remote sensing images derived from denseunet. Remote Sensing 11, 2499. https://doi.org/10.3390/rs11212499.
Xu, R., He, C., Liu, X., Chen, D., Qin, Q., 2017a. Bayesian fusion of multi-scale detectors for road extraction from Sar images. ISPRS Int. J. Geo-Inf. 6 (1), 26. https://doi.org/10.3390/ijgi6010026.
Xu, S., Wang, R., Zheng, H., 2017b. Road curb extraction from mobile lidar point clouds. IEEE Trans. Geosci. Remote Sens. 55, 996–1009. https://doi.org/10.1109/TGRS.2016.2617819.
Xu, Y., Xie, Z., Feng, Y., Chen, Z., 2018. Road extraction from high-resolution remote sensing imagery using deep learning. Remote Sensing 10, 1461. https://doi.org/10.3390/rs10091461.
Xu, Z., Shen, Z., Li, Y., Xia, L., Wang, H., Li, S., Jiao, S., Lei, Y., 2021. Road extraction in mountainous regions from high-resolution images based on dsdnet and terrain optimization. Remote Sensing 13, 90. https://doi.org/10.3390/rs13010090.
Yadav, M., 2021. A multi-constraint combined method for road extraction from airborne laser scanning data. Measurement 186. https://doi.org/10.1016/j.measurement.2021.110077.
Yadav, M., Singh, A.K., Lohani, B., 2017. Extraction of road surface from mobile lidar data of complex road environment. Int. J. Remote Sens. 38, 4645–4672. https://doi.org/10.1080/01431161.2017.1320451.
Yadav, M., Singh, A.K., 2017. Rural road surface extraction using mobile lidar point cloud data. J. Indian Soc. Remote Sens. 46, 531–538. https://doi.org/10.1007/s12524-017-0732-4.
Yang, B., Dong, Z., Liu, Y., Liang, F., Wang, Y., 2017a. Computing multiple aggregation levels and contextual features for road facilities recognition using mobile laser scanning data. ISPRS J. Photogramm. Remote Sens. 126, 180–194. https://doi.org/10.1016/J.ISPRSJPRS.2017.02.014.
Yang, B., Fang, L., Li, J., 2013. Semi-automated extraction and delineation of 3d roads of street scene from mobile laser scanning point clouds. ISPRS J. Photogramm. Remote Sens. 79, 80–93. https://doi.org/10.1016/j.isprsjprs.2013.01.016.
Yang, B., Liu, Y., Dong, Z., Liang, F., Li, B., Peng, X., 2017b. 3d Local feature Bkd to extract road information from mobile laser scanning point clouds. ISPRS J. Photogramm. Remote Sens. 130, 329–343. https://doi.org/10.1016/j.isprsjprs.2017.06.007.
Yang, B., Wei, Z., Li, Q., Li, J., 2012. Automated extraction of street-scene objects from mobile lidar point clouds. Int. J. Remote Sens. 33, 5839–5861. https://doi.org/10.1080/01431161.2012.674229.
Yang, C., Zhu, L., Ai, Y., 2019a. Analysis of model optimization strategies for a low-resolution camera-lidar fusion based road detection network. In: Paper presented at the 2019 Chinese Automation Congress (CAC), Hangzhou, China, 22-24 Nov. 2019. 10.1109/CAC48633.2019.8997471.
Yang, F., Wang, H., Jin, Z., 2020. A fusion network for road detection via spatial propagation and spatial transformation. Pattern Recogn. 100, 107141 https://doi.org/10.1016/j.patcog.2019.107141.
Yang, X., Li, X., Ye, Y., Lau, R.Y., Zhang, X., Huang, X., 2019b. Road detection and centerline extraction via deep recurrent convolutional neural network U-net. IEEE Trans. Geosci. Remote Sens. 57 (9), 7209–7220. https://doi.org/10.1109/TGRS.2019.2912301.

Yin, D., Du, S., Wang, S., Guo, Z., 2016. A direction-guided ant colony optimization method for extraction of urban road information from very-high-resolution images. IEEE J. Sel. Top. Appl. Earth Obs. Remote Sens. 8 (10), 4785–4794. https://doi.org/10.1109/JSTARS.2015.2477097.

Yu, D., Xiong, H., Xu, Q., Wang, J., Li, K., 2019. Multi-stage residual fusion network for lidar-camera road detection. In: Paper presented at the 2019 IEEE Intelligent Vehicles Symposium (IV), Paris, France, 9-12 June 2019. 10.1109/IVS.2019.8813983.

Yuan, J., Wang, D., Wu, B., Yan, L., Li, R., 2011. Legion-based automatic road extraction from satellite imagery. IEEE Trans. Geosci. Remote Sens. 49, 4528–4538. https://doi.org/10.1109/TGRS.2011.2146785.

Zai, D., Li, J., Guo, Y., Cheng, M., Lin, Y., Luo, H., 2018. 3-D road boundary extraction from mobile laser scanning data via supervoxels and graph cuts. IEEE Trans. Intell. Transp. Syst. 19, 802–813. https://doi.org/10.1109/TITS.2017.2701403.

Zang, Y., Wang, C., Cao, L., Yu, Y., Li, J., 2016. Road network extraction via aperiodic directional structure measurement. IEEE Trans. Geosci. Remote Sens. 54 (6), 3322–3335. https://doi.org/10.1109/TGRS.2016.2514602.

Zang, Y., Wang, C., Yu, Y., Luo, L., Yang, K., Li, J., 2017. Joint enhancing filtering for road network extraction. IEEE Trans. Geosci. Remote Sens. 55 (3), 1511–1525. https://doi.org/10.1109/TGRS.2016.2626378.

Zeng, T., Gao, Q., Ding, Z., Chen, J., Li, G., 2019. Road network extraction from low-contrast sar images. IEEE Geosci. Remote Sens. Lett. 16, 907–911. https://doi.org/10.1109/LGRS.2018.2889299.

Zhang, J., Chen, L., Wang, C., Zhuo, L., Tian, Q., Liang, X., 2017. Road recognition from remote sensing imagery using incremental learning. IEEE Trans. Intell. Transp. Syst. 18, 2993–3005. https://doi.org/10.1109/TITS.2017.2665658.

Zhang, J., Hu, Q., Li, J., Ai, M., 2021. Learning from Gps trajectories of floating car for Cnn-based urban road extraction with high-resolution satellite imagery. IEEE Trans. Geosci. Remote Sens. 59, 1836–1847. https://doi.org/10.1109/TGRS.2020.3003425.

Zhang, Q., Kong, Q., Zhang, C., You, S., Wei, H., Sun, R., Li, L., 2019a. A new road extraction method using Sentinel-1 Sar images based on the deep fully convolutional neural network. European Journal of Remote Sensing 52 (1), 572–582. https://doi.org/10.1080/22797254.2019.1694447.

Zhang, W., 2010. Lidar-based road and road-edge detection," In: Paper presented at the IEEE Intelligent Vehicles Symposium (IV), San Diego, CA, USA, 21–24 June 2010. 10.1109/IVS.2010.5548134.

Zhang, X., Ma, W., Li, C., Wu, J., Tang, X., Jiao, L., 2020. Fully convolutional network-based ensemble method for road extraction from aerial images. IEEE Geosci. Remote Sens. Lett. 17, 1777–1781. https://doi.org/10.1109/LGRS.2019.2953523.

Zhang, Y., Xiong, Z., Zang, Y., Wang, C., Li, J., Li, X., 2019b. Topology-aware road network extraction via multi-supervised generative adversarial networks. Remote Sensing 11 (9), 1017. https://doi.org/10.3390/RS11091017.

Zhang, Y., Xia, G., Wang, J., Lha, D., 2019c. A multiple feature fully convolutional network for road extraction from high-resolution remote sensing image over mountainous areas. IEEE Geosci. Remote Sens. Lett. 16 (10), 1600–1604. https://doi.org/10.1109/LGRS.2019.2905350.

Zhang, Y., Zhang, J., Li, T., Sun, K., 2016. Road extraction and intersection detection based on tensor voting. In: Paper presented at the 2016 IEEE International Geoscience and Remote Sensing Symposium (IGARSS), Beijing, China, July 2016. 10.1109/IGARSS.2016.7729405.

Zhang, Y., Wang, J., Wang, X., Dolan, J.M., 2018a. Road-segmentation-based curb detection method for self-driving via a 3d-Lidar sensor. IEEE Trans. Intell. Transp. Syst. 19 (12), 3981–3991. https://doi.org/10.1109/TITS.2018.2789462.

Zhang, Y., Gu, S., Yang, J., Álvarez, J., Kong, H., 2018b. Fusion of Lidar and camera by scanning in lidar imagery and image-guided diffusion for urban road detection. In: Paper presented at the 2018 IEEE Intelligent Vehicles Symposium (IV), Changshu, China, 26-30 June 2018. 10.1109/IVS.2018.8500401.

Zhang, Z., Liu, Q., Wang, Y., 2018c. Road extraction by deep residual U-net. IEEE Geosci. Remote Sens. Lett. 15 (5), 749–753. https://doi.org/10.1109/LGRS.2018.2802944.

Zhang, Z., Zhang, X., Sun, Y., Zhang, P., 2018d. Road centerline extraction from very-high-resolution aerial image and lidar data based on road connectivity. Remote Sensing 10 (8), 1284. https://doi.org/10.3390/rs10081284.

Zhang, Z., Wang, Y., 2019. Jointnet: A common neural network for road and building extraction. Remote Sens. 11, 696. https://doi.org/10.3390/rs11060696.

Zhang, Z., Miao, C., Liu, C.a., Tian, Q., 2022. Dcs-transupernet: road segmentation network based on Cswin transformer with dual resolution. Appl. Sci. 12(7), 3511. 10.3390/app12073511.

Zhao, H., Shi, J., Qi, X., Wang, X., Jia, J., 2017. Pyramid scene parsing network. In: Paper presented at the 2017 IEEE Conference on Computer Vision and Pattern Recognition (CVPR), Honolulu, HI, USA, 21-26 July 2017. 10.1109/cvpr.2017.660.

Zhao, J., You, S., Huang, J., 2011. Rapid extraction and updating of road network from airborne lidar data. Paper presented at the 2011 IEEE Applied Imagery Pattern Recognition Workshop (AIPR), 11–13 Oct. 10.1109/AIPR.2011.6176360.

Zhao, J., You, S., 2012. Road Network Extraction from Airborne Lidar Data Using Scene Context. In: Paper presented at the 2012 IEEE Computer Society Conference on Computer Vision and Pattern Recognition Workshops, 16-21 June 2012. 156.10.1109/CVPRW.2012.6238909.

Zhao, L., Yan, L., Meng, X., 2021. The extraction of street curbs from mobile laser scanning data in urban areas. Remote Sens. 13 (12), 2407. https://doi.org/10.3390/rs13122407.

Zheng, J., Yang, S., Wang, X., Xia, X., Xiao, Y., Li, T., 2019. A decision tree based road recognition approach using roadside fixed 3d lidar sensors. IEEE Access 7, 53878-53890. 170.10.1109/ACCESS.2019.2912581.

Zhou, G., Chen, W., Gui, Q., Li, X., Wang, L., 2022. Split depth-wise separable graph-convolution network for road extraction in complex environments from high-resolution remote-sensing images. IEEE Trans. Geosci. Remote Sens. 60, 1–15. https://doi.org/10.1109/tgrs.2021.3128033.

Zhou, H., Kong, H., Wei, L., Creighton, D., Nahavandi, S., 2017. On detecting road regions in a single Uav image. IEEE Trans. Intell. Transp. Syst. 18 (99), 1713–1722. https://doi.org/10.1109/TITS.2016.2622280.

Zhou, M., Sui, H., Chen, S., Wang, J., Chen, X., 2020. Bt-Roadnet: a boundary and topologically-aware neural network for road extraction from high-resolution remote sensing imagery. ISPRS J. Photogramm. Remote Sens. 168, 288–306. https://doi.org/10.1016/j.isprsjprs.2020.08.019.

Zhou, T., Sun, C., Fu, H., 2019. Road information extraction from high-resolution remote sensing images based on road reconstruction. Remote Sensing 11, 79. https://doi.org/10.3390/rs11010079.

Zhou, Z., Siddiquee, M.M.R., Tajbakhsh, N., Liang, J., 2018. Unet++: A Nested U-Net Architecture for Medical Image Segmentation. In: Deep Learning in Medical Image Analysis and Multimodal Learning for Clinical Decision Support: Springer, vol. 11045, pp. 3-11. 10.1007/978-3-030-00889-5_1.

Zhu, Q., Zhang, Y., Wang, L., Zhong, Y., Guan, Q., Lu, X., Zhang, L.-P., Li, D., 2021. A global context-aware and batch-independent network for road extraction from Vhr satellite imagery. ISPRS J. Photogramm. Remote Sens. 175, 353–365. https://doi.org/10.1016/J.ISPRSJPRS.2021.03.016.

Ziems, M., Rottensteiner, F., Heipke, C., 2017. Verification of road databases using multiple road models. ISPRS J. Photogramm. Remote Sens. 130, 44–62. https://doi.org/10.1016/J.ISPRSJPRS.2017.05.005.